Polyblock Algorithm-Based Robust Beamforming for Downlink Multi-User Systems With Per-Antenna Power Constraints

Ming Ding, *Member, IEEE*, Hanwen Luo, and Wen Chen, *Senior Member, IEEE*

Abstract—In this paper, we investigate the robust beamforming for multi-user multiple-input single-output systems under quantized channel direction information (CDI) with per-antenna power constraints. The robustness of the considered beamforming design is achieved in the sense that the stochastic interference leakage is below a certain level by a given probability. Our design objective is to maximize the expectation of the weighted sum-rate performance. From the discussion of the non-robust optimal beamforming based on the polyblock algorithm, we propose a robust beamforming scheme for the quantized CDI case with per-antenna power constraints. In the proposed beamforming scheme, we use Jensen's inequality to generate a tractable feasibility problem for the polyblock algorithm and apply the semi-definite programming relaxation, as well as the randomization technique to find its approximate rank-one matrix solution and user equipments' beamforming vectors. Simulation results show that substantial gains can be achieved by the proposed scheme compared with the existing schemes in terms of the average weighted sum-rate performance. Although very high complexity is required for the implementation of the proposed scheme, it stands as a good benchmark for robust beamforming designs.

Index Terms—Multi-user, robust beamforming, per-antenna power constraints, quantized CDI, polyblock algorithm, weighted sum-rate.

I. INTRODUCTION

MULTI-USER (MU) space division multiple access (SDMA) schemes are extremely attractive in an infrastructure-based network, where powerful nodes such as multi-antenna base stations (BSs) provide service to multiple user equipments (UEs) with limited signal processing capability and a small number of antennas, because MU SDMA can offer both spatial multiplexing and multi-user diversity gains [1]. In a multi-antenna broadcast channel (BC) model

M. Ding is with Sharp Laboratories of China Co., Ltd., Shanghai 201203, China (e-mail: ming.ding@cn.sharp-world.com).

H. Luo is with the College of Information, Mechanical and Electrical Engineering, Shanghai Normal University, Shanghai 200234, China, and also with the Department of Electronic Engineering, Shanghai Jiao Tong University, Shanghai 200240, China (e-mail: h6293@126.com).

W. Chen is with the School of Electronic Engineering and Automation, Guilin University of Electronic Technology, Guilin 541004, China, and the Department of Electronic Engineering, Shanghai Jiao Tong University, Shanghai 200240, China (e-mail: wenchen@sjtu.edu.cn).

with MU SDMA, the multiplexing gain can be achieved by MU transmissions with the dirty paper coding technique [2] or linear transmit beamforming, e.g., the zero-forcing (ZF) beamforming [3]. Moreover, when the UE number is large, the capacity of the BC system also grows with the UE number according to a double logarithm scaling law thanks to the multi-UE diversity gain [4].

However, all these promising results are predicated on the assumption of perfect channel direction information (CDI) available at the BS, which is too ideal for practical systems, especially for the frequency division duplex (FDD) systems such as the fourth generation (4G) cellular networks, e.g., the Long Term Evolution Advanced (LTE-A) FDD system [5]. In order to harvest a large portion of the performance gain offered by MU SDMA, a lot of work has been devoted to ensure the accuracy of CDI in practical networks. For example, the feedback periodicity of CDI can be configured to be a few tens of milliseconds for an LTE-A UE [5], which is significantly smaller than the coherence time of a low-speed UE's channel impulse response, so that UE's reported CDI will not be outdated when the BS scheduler consults it. However, the issue of CDI quantization errors, which is caused by the CDI quantization process performed by each UE for limited-bit feedback [6], remains to be a serious problem even in the state-of-the-art networks.

The existence of CDI quantization errors motivates the design of robust beamforming schemes, which take the uncertain channel distortions into account. In [7], the authors proposed a robust beamforming scheme for an MU multi-antenna BC system to minimize the transmission power while maintaining certain quality of service (QoS) requirements. In [8], the authors investigated robust beamforming schemes to minimize the sum of UEs' mean squared errors (MSEs). Based on inter-UE interference leakage control [9], the authors in [10] designed a robust beamforming scheme, which maximizes a lower bound for each UE's average signal-to-leakage-plus-noise ratio (SLNR). Recently, in [11] and [12], the authors proposed a robust leakage-based transmit beamforming scheme, which implicitly optimizes UE's average signal-to-interference-plus-noise ratio (SINR) by maximizing the average signal power subject to probabilistic leakage constraints. Furthermore, robust beamforming has been extended to more sophisticated models such as the multiple-input multiple-output (MIMO) relay networks [13], [14] and the multi-cell coordinated beamforming scenarios [15], [16], etc.

In this paper, we further investigate the robust beamforming schemes. In particular, we consider a beamforming problem with a more realistic power constraint that limits the transmission power at the BS on a per-antenna basis. Comparing with the existing robust beamforming schemes, our assumption on the transmission power is more practical since each antenna of the multi-antenna BS or a distributed antenna system is usually equipped with an individual power amplifier at its analog front-end [17]. Besides, our design objective is to maximize the weighted sum-rate performance. Although minimization of MSE or bit error rate (BER) is also a well-motivated design objective [8], it is usually not the direct goal for network optimization [18]. In the modern wireless communication networks, e.g., the LTE-A system, the adaptive modulation and coding (MC) technology has been widely employed, in which the target of the expected MSE or BER is normally preset by the network but the payload size is adjustable by MC schemes [19]. For example, the data-packet error rate is loosely controlled around 0.1 in the LTE-A network [5], which is achieved by employing rate adaptation algorithms. Therefore, instead of decreasing the MSE or BER, increasing the sum throughput or the weighted sum throughput with consideration of UE fairness, is the top priority in network optimization [18]. Hence, the weighted sum-rate performance [20] is an extremely useful design goal because it can provide an achievable upper-bound for the weighted sum throughput for the BC systems.

In this paper, we propose a robust beamforming scheme based on the polyblock algorithm [21] (see Appendix I for details) by maximizing an upper-bound for the weighted sum-rate performance under per-antenna power constraints. It should be noted that recently the polyblock algorithm [21] has been applied to a general K-user Gaussian interference channel (GIC) system to solve the weighted sum-rate maximization problem under the condition of perfect CDI [22]. The Algorithm 1 in [22] bears close similarity to the polyblock algorithm introduced in Appendix I [21], but with more complicated expressions of per-UE SINR. Our main contribution in this paper is to extend the framework developed in [21] and [22] to the robust beamforming design with consideration of CDI quantization errors. To accomplish this, we characterize a feasible rate tuple and formulate a robust beamforming problem, the robustness of which is achieved in a similar sense as in [11] that the uncertain interference leakage due to CDI quantization errors should be below a certain level by a given probability. In order to solve the proposed robust beamforming problem, we use the Jensen's inequality to generate a tractable feasibility problem for the polyblock algorithm and apply the semi-definite programming (SDP) relaxation as well as the randomization technique to find its approximate rank-one matrix solution and UEs' beamforming vectors.

The rest of the paper is organized as follows. Section II addresses the system model and the formulation of CDI quantization errors. Section III discusses the non-robust beamforming schemes. Section IV presents the proposed robust beamforming scheme. The paper is completed with simulation results and conclusions in Sections V and VI, respectively.

Notations: $(\cdot)^{\mathrm{T}}$, $(\cdot)^{\mathrm{H}}$, $(\cdot)^{-1}$, $(\cdot)^{\dagger}$, $\mathrm{tr}\{\cdot\}$, and $\mathrm{rank}\{\cdot\}$ stand for the transpose, conjugate transpose, inverse, pseudo-inverse,
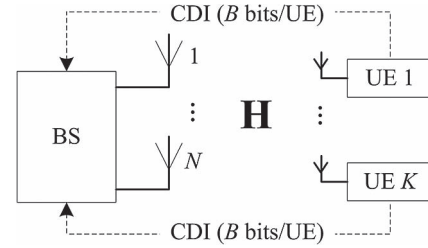

Fig. 1.   Illustration of a downlink MU-MISO system with limited-bit CDI.

trace and rank of a matrix, respectively. $\mathbf{I}_N$ stands for an $N \times N$ identity matrix. $\mathbf{A}_{i,:}$, $\mathbf{A}_{:,j}$, and $\mathbf{A}_{i,j}$ denote the i-th row, j-th column and (i,j)-th entry of matrix $\mathbf{A}$. Besides, $\mathbf{A} \succeq 0$ and $\mathbf{A} \in \mathbb{H}_N^+$ mean that matrix $\mathbf{A}$ is positive semi-definite and $\mathbf{A}$ is an N by N positive semi-definite Hermitian matrix, respectively. $\|\mathbf{a}\|$ and $\mathbf{a}_i$ denotes the Euclidean norm and the i-th element of vector $\mathbf{a}$. For any two vectors $\mathbf{a}, \mathbf{b} \in \mathbb{R}^n$, we write $\mathbf{a} \leq \mathbf{b}$ to indicate that $\mathbf{a}_i \leq \mathbf{b}_i$, $\forall i \in \{1, 2, \ldots, n\}$. $\mathbb{E}_{[\mathbf{x}]}\{\cdot\}$ and $\Re\{\cdot\}$ denote the expectation operation over a random vector $\mathbf{x}$ and the real part of a complex value, respectively. C_j^i counts the combinations of choosing i elements from a set of j elements. $\mathcal{N}(\mathbf{0}, \mathbf{X})$ represents a circularly symmetric complex Gaussian distribution with mean of zero vector and covariance matrix $\mathbf{X}$. Finally, $\Pr(x)$ denotes the probability of event x.

II. SYSTEM MODEL

In this paper, we consider a downlink MU-MISO system with limited-bit CDI feedback as illustrated in Fig. 1, where a BS or a distributed antenna system is equipped with N transmit antennas, and K single-antenna UEs receive data transmissions from the BS simultaneously.

In Fig. 1, it requires $N \geq K$ to support K independent data streams. However, our results can be easily extended to the case of $N < K$ with UE selection performed at the BS [23]. We assume that all channels experience independently identical distribution (i.i.d.) Rayleigh flat fading and remain unchanged during the MU-MISO transmission. Besides, the base-band channel vector between the BS and the k-th UE $(k \in \{1, 2, \ldots, K\})$ is denoted as $\mathbf{h}_k \in \mathbb{C}^{1 \times N}$.

In practice, perfect channel state information (CSI) of $\mathbf{h}_k$ is usually not available at the BS side. Hence, in Fig. 1 we assume imperfect CDI for the downlink MU-MISO system, where each UE quantizes its CDI and feeds it back to the BS with B bits. Here, the CDI refers to the normalized channel vector of UE k denoted as $\tilde{\mathbf{h}}_k = \mathbf{h}_k / \|\mathbf{h}_k\|$. We assume that the quantized CDI is defined as the index of a vector $\hat{\mathbf{h}}_k$ chosen from a random vector quantization (RVQ) codebook $\mathbf{C}_k = \{\mathbf{c}_{k,1}, \mathbf{c}_{k,2}, \ldots, \mathbf{c}_{k,2^B}\}$ to match $\tilde{\mathbf{h}}_k$ [24]. The codebook $\mathbf{C}_k$ consists of 2^B unit vectors $\mathbf{c}_{k,i}$ $(i \in \{1, 2, \ldots, 2^B\})$ isotropically distributed in $\mathbb{C}^{1 \times N}$ and $\hat{\mathbf{h}}_k$ is selected as

$$\hat{\mathbf{h}}_k = \arg\max_{\mathbf{c}_{k,i} \in \mathbf{C}_k} \left| \mathbf{c}_{k,i} \tilde{\mathbf{h}}_k^{\mathrm{H}} \right|. \tag{1}$$

Then $\tilde{\mathbf{h}}_k$ can be decomposed as [6]

$$\tilde{\mathbf{h}}_k = \cos\left(\angle(\tilde{\mathbf{h}}_k, \hat{\mathbf{h}}_k)\right) \hat{\mathbf{h}}_k + \sin\left(\angle\left(\tilde{\mathbf{h}}_k, \hat{\mathbf{h}}_k\right)\right) \mathbf{e}_k, \tag{2}$$

where $\mathbf{e}_k$ is a quantization error vector orthogonal to $\hat{\mathbf{h}}_k$. Note that the instantaneous channel magnitude information (CMI), i.e., $\|\mathbf{h}_k\|^2$, is a scalar and can be quantized easily [16]. In our simulations, we will show that even with average CMI only, i.e., $\mathbb{E}_{[\mathbf{h}_k]}\{\|\mathbf{h}_k\|^2\}$, the performance of the interested beamforming schemes is comparable with that achieved by perfect CMI. Therefore, in the following we concentrate on quantized CDI and assume average CMI at the BS. For notational brevity, we denote $A_k^{\mathrm{ave}} = \mathbb{E}_{[\mathbf{h}_k]}\{\|\mathbf{h}_k\|^2\}$ hereafter.

Let $\mathbf{w}_k \in \mathbb{C}^{N \times 1}$ be the beamforming vector for UE k, then the signal received at UE k can be written as

$$
\begin{aligned}
y_k &= \mathbf{h}_k \mathbf{w}_k x_k + \sum_{j=1, j \neq k}^{K} \mathbf{h}_k \mathbf{w}_j x_j + n_k \\
&= \mathbf{h}_k \mathbf{W} \mathbf{x} + n_k,
\end{aligned}
\tag{3}
$$

where $\mathbf{x} = [x_1, x_2, \ldots, x_K]^{\mathrm{T}}$ and x_k is the data symbol intended for UE k. Without loss of generality, we assume that $\mathbf{x}$ satisfies $\mathbb{E}_{[\mathbf{x}]}\{\mathbf{x}\mathbf{x}^{\mathrm{H}}\} = \mathbf{I}_K$. n_k is a zero-mean circularly symmetric complex Gaussian (ZMCSCG) noise variable with $\mathbb{E}_{[n_k]}\{n_k n_k^{\mathrm{H}}\} = N_0$. In addition, $\mathbf{W} = [\mathbf{w}_1, \mathbf{w}_2, \ldots, \mathbf{w}_K]$ and it is subject to an average per-antenna transmit power constraint expressed as

$$
\begin{aligned}
\mathbb{E}_{[\mathbf{x}]}\left\{\left[\mathbf{W}\mathbf{x}(\mathbf{W}\mathbf{x})^{\mathrm{H}}\right]_{n,n}\right\} &= \mathrm{tr}\{\mathbf{W}\mathbf{W}^{\mathrm{H}}\mathbf{A}_n\} \\
&\leq P_n,
\end{aligned}
\tag{4}
$$

where $\mathbf{A}_n$ $(n \in \{1, 2, \ldots, N\})$ is an N by N zero matrix except that the n-th diagonal element $(\mathbf{A}_n)_{n,n} = 1$ and P_n is the maximum transmission power of the n-th BS antenna. The sum of P_n is denoted as the BS's maximum transmission power P, i.e., $P = \sum_{n=1}^{N} P_n$. By stacking the received signals of all UEs, we have

$$
\mathbf{y} = \mathbf{H}\mathbf{W}\mathbf{x} + \mathbf{n},
\tag{5}
$$

where $\mathbf{y} = [y_1, y_2, \ldots, y_K]^{\mathrm{T}}$, $\mathbf{H} = [\mathbf{h}_1^{\mathrm{T}}, \mathbf{h}_2^{\mathrm{T}}, \ldots, \mathbf{h}_K^{\mathrm{T}}]^{\mathrm{T}}$ and $\mathbf{n} = [n_1, n_2, \ldots, n_K]^{\mathrm{T}}$.

III. NON-ROBUST BEAMFORMING SCHEMES

For non-robust beamforming schemes, channel uncertainties due to CDI quantization errors are ignored [22], [25], [26]. Therefore, at the BS side, each UE's available channel vector information is expressed by $\check{\mathbf{h}}_k = \sqrt{A_k^{\mathrm{ave}}}\hat{\mathbf{h}}_k$. In this section, we first discuss the non-robust ZF beamforming scheme with per-antenna power constraints, the results of which will serve as the benchmark for performance comparison. Then we introduce the non-robust optimal beamforming scheme with per-antenna power constraints, which will lead to our robust beamforming design to be addressed in the next section.

A. The Non-Robust ZF Beamforming Scheme With Per-Antenna Power Constraints

The ZF beamforming is a well-known design for the downlink MU-MISO system, which aims to fully mitigate the inter-UE interference. Considering the maximization of the weighted sum-rate for an MU-MISO system, the authors of [25] ad-

dressed that the solution of the non-robust ZF beamforming under per-antenna power constraints, called the ZF-PA scheme in the sequel, should be found by solving a standard semi-definite programming (SDP) problem shown as

$$
\max_{\mathbf{Q}_k \in \mathbb{H}_N^+} \quad f(\{\mathbf{Q}_k\}) = \sum_{k=1}^{K} \alpha_k \log_2 \left(1 + \frac{\check{\mathbf{h}}_k \mathbf{Q}_k \check{\mathbf{h}}_k^{\mathrm{H}}}{N_0}\right)
$$

$$
\text{s.t.} \quad \mathrm{tr}\{\mathbf{Q}_k \check{\mathbf{h}}_j^{\mathrm{H}} \check{\mathbf{h}}_j\} = 0, \quad j \in \{1, \ldots, K\} \text{ and } j \neq k;
$$

$$
\sum_{k=1}^{K} \mathrm{tr}\{\mathbf{Q}_k \mathbf{A}_n\} \leq P_n, \quad n \in \{1, \ldots, N\},
\tag{6}
$$

where α_k is the weight on UE k's rate and $\mathbf{Q}_k = \mathbf{w}_k \mathbf{w}_k^{\mathrm{H}}$. The first and second sets of constraints in problem (6) represent the requirements of zero interference among UEs and per-antenna power limitation, respectively. Problem (6) is a convex optimization problem and its numerical solution can be obtained by the use of standard mathematical software [27]. Note that for the beamforming operation, an additional non-convex rank-one constraint should be imposed on each $\mathbf{Q}_k$. Fortunately, it has been proven in [25] that problem (6) always admits a solution with rank-one matrices. Thus, such rank-one constraints have been omitted in problem (6). Suppose that $\{\mathbf{Q}_k^{\mathrm{ZF\text{-}PA}}\}$ is such rank-one matrix solution and $\mathbf{Q}_k^{\mathrm{ZF\text{-}PA}} = \mathbf{q}_k^{\mathrm{ZF\text{-}PA}}(\mathbf{q}_k^{\mathrm{ZF\text{-}PA}})^{\mathrm{H}}$, then the beamforming vector for UE k in the ZF-PA scheme becomes $\mathbf{w}_k^{\mathrm{ZF\text{-}PA}} = \mathbf{q}_k^{\mathrm{ZF\text{-}PA}}$.

B. The Non-Robust Optimal Beamforming With Per-Antenna Power Constraints

As for the non-robust optimal beamforming, we should directly maximize the weighted sum-rate under per-antenna power constraints, which will be referred to as the NROpt-PA scheme in the following. The corresponding optimization problem can be established as

$$
\max_{\mathbf{Q}_k \in \mathbb{H}_N^+} \quad f(\{\mathbf{Q}_k\}) = \sum_{k=1}^{K} \alpha_k \log_2 \left(1 + \frac{\check{\mathbf{h}}_k \mathbf{Q}_k \check{\mathbf{h}}_k^{\mathrm{H}}}{\sum_{j \neq k} \check{\mathbf{h}}_k \mathbf{Q}_j \check{\mathbf{h}}_k^{\mathrm{H}} + N_0}\right)
$$

$$
\text{s.t.} \quad \sum_{k=1}^{K} \mathrm{tr}\{\mathbf{Q}_k \mathbf{A}_n\} \leq P_n, \quad n \in \{1, \ldots, N\};
$$

$$
\mathrm{rank}\{\mathbf{Q}_k\} = 1, \quad k \in \{1, \ldots, K\}.
\tag{7}
$$

In problem (7), $f(\{\mathbf{Q}_k\})$ can also be redefined as $g(\hat{\mathbf{r}}) = \sum_{k=1}^{K} \alpha_k \hat{r}_k$ with regard to a vector $\hat{\mathbf{r}} = (\hat{r}_1, \hat{r}_2, \ldots, \hat{r}_K)$, where $\hat{r}_k$ is the BS's estimation on the rate of UE k defined as $\hat{r}_k = \log_2(1 + (\check{\mathbf{h}}_k \mathbf{Q}_k \check{\mathbf{h}}_k^{\mathrm{H}}/(\sum_{j \neq k} \check{\mathbf{h}}_k \mathbf{Q}_j \check{\mathbf{h}}_k^{\mathrm{H}} + N_0)))$. Suppose that $\mathbf{Q}_k^{\mathrm{NROpt\text{-}PA}} = \mathbf{q}_k^{\mathrm{NROpt\text{-}PA}}(\mathbf{q}_k^{\mathrm{NROpt\text{-}PA}})^{\mathrm{H}}$ is the solution to problem (7). Then the beamforming vector for UE k can be written as $\mathbf{w}_k^{\mathrm{NROpt\text{-}PA}} = \mathbf{q}_k^{\mathrm{NROpt\text{-}PA}}$.

Unfortunately, problem (7) is non-convex and cannot be solved in a straightforward way. Nevertheless, the maximum value of $f(\{\mathbf{Q}_k\})$ does exist since the UE rate region of problem (7) is bounded. This is because that the per-antenna

transmission powers are strictly limited and the noise has a non-zero power so that each UE's rate is bounded even if no inter-UE interference exists. In [20] and [26], the authors addressed that problem (7) is a monotonic optimization problem because $g(\hat{\mathbf{r}}^{(1)}) \leq g(\hat{\mathbf{r}}^{(2)})$ for any $\hat{\mathbf{r}}^{(1)} \leq \hat{\mathbf{r}}^{(2)}$. Thus, it can be solved using the polyblock algorithm [21], [22], which guarantees the convergence and global optimality of the solution. The basic idea of the polyblock algorithm is to gradually refine the outer boundary of the feasible region, thereby the upper-bound for the objective function will decrease continuously. The process is terminated when the upper-bound is achievable with a gap of ε, where ε is the optimality tolerance parameter, taking a reasonably small value. Details of the polyblock algorithm to solve problem (7) is relegated to Appendix I.

IV. THE PROPOSED ROBUST BEAMFORMING WITH PER-ANTENNA POWER CONSTRAINTS

In this section, we propose to adapt the NROpt-PA scheme [21], [22] discussed in Section III-B for the case of quantized CDI. As a result, we should take imperfect CDI into account when designing UEs' beamforming vectors. To be more specific, at the BS side, instead of using $\hat{\mathbf{h}}_k$ as the substitution for $\tilde{\mathbf{h}}_k$, $\tilde{\mathbf{h}}_k$ should be considered as a randomly-reconstructed normalized channel vector $\tilde{\mathbf{h}}_k^\diamond$, which is isotropically distributed around $\hat{\mathbf{h}}_k$.

A. Problem Formulation

Similar to (2), the randomly-reconstructed normalized channel vector $\tilde{\mathbf{h}}_k^\diamond$ distributed around $\hat{\mathbf{h}}_k$ can be expressed as [6]

$$\tilde{\mathbf{h}}_k^\diamond = \sqrt{1 - Z}\hat{\mathbf{h}}_k + \sqrt{Z}\mathbf{e}_k^\diamond, \tag{8}$$

where $\mathbf{e}_k^\diamond$ is isotropically distributed in the $(N-1)$-dimensional nullspace of $\hat{\mathbf{h}}_k$ and the random variable Z is defined as $Z = \sin^2(\angle(\tilde{\mathbf{h}}_k^\diamond, \hat{\mathbf{h}}_k))$. According to [6], when a RVQ codebook is considered, Z follows the distribution of the minimum variable of 2^B i.i.d. beta$(N-1, 1)$ random variables.

Since the deterministic expression of the performance measure $f(\{\mathbf{Q}_k\})$ in problem (7) is no longer available due to the uncertainties in $\tilde{\mathbf{h}}_k^\diamond$, it is logical to optimize the expectation of $f(\{\mathbf{Q}_k\})$ over $[\tilde{\mathbf{h}}_k^\diamond|\hat{\mathbf{h}}_k]$ $(k \in \{1, \ldots, K\})$, i.e., $\mathbb{E}_{[\tilde{\mathbf{h}}_k^\diamond|\hat{\mathbf{h}}_k]}\{f(\{\mathbf{Q}_k\})\}$, which can be computed according to the objective function in problem (7) as,

$$\mathbb{E}_{[\tilde{\mathbf{h}}_k^\diamond|\hat{\mathbf{h}}_k]}\{f(\{\mathbf{Q}_k\})\}$$

$$= \sum_{k=1}^{K} \alpha_k \mathbb{E}_{[\tilde{\mathbf{h}}_k^\diamond|\hat{\mathbf{h}}_k]}\{\log_2(1 + SINR_k^\diamond)\}, \tag{9}$$

where

$$SINR_k^\diamond = \frac{A_k^{\mathrm{ave}}\tilde{\mathbf{h}}_k^\diamond \mathbf{Q}_k \tilde{\mathbf{h}}_k^{\diamond\mathrm{H}}}{A_k^{\mathrm{ave}}\sum_{j \neq k}\tilde{\mathbf{h}}_k^\diamond \mathbf{Q}_j \tilde{\mathbf{h}}_k^{\diamond\mathrm{H}} + N_0}. \tag{10}$$

For brevity, we omit the subscription $[\tilde{\mathbf{h}}_k^\diamond|\hat{\mathbf{h}}_k]$ of $\mathbb{E}$ hereafter if the expectation operation is conducted over $[\tilde{\mathbf{h}}_k^\diamond|\hat{\mathbf{h}}_k]$. In the

respect of maximizing (9), the problem of the optimal robust beamforming with per-antenna power constraints is cast as

$$\max_{\mathbf{Q}_k \in \mathbb{H}_N^+} \quad \mathbb{E}\{f(\{\mathbf{Q}_k\})\}$$

$$\mathrm{s.t.} \quad \sum_{k=1}^{K}\mathrm{tr}\{\mathbf{Q}_k\mathbf{A}_n\} \leq P_n, \quad n \in \{1, \ldots, N\};$$

$$\mathrm{rank}\{\mathbf{Q}_k\} = 1, \quad k \in \{1, \ldots, K\}. \tag{11}$$

However, it is very difficult to handle problem (11) because (9) has no explicit expression. Here, we consider its upper-bound given by the Jensen's inequality as

$$\mathbb{E}\{\log_2(1 + SINR_k^\diamond)\} \leq \log_2(1 + \mathbb{E}\{SINR_k^\diamond\}). \tag{12}$$

Based on (12), we can transform problem (11) into the following problem by maximizing the upper-bound for $\mathbb{E}\{f(\{\mathbf{Q}_k\})\}$.

$$\max_{\mathbf{Q}_k \in \mathbb{H}_N^+} \quad \tilde{f}(\{\mathbf{Q}_k\}) = \sum_{k=1}^{K}\alpha_k\log_2(1 + \mathbb{E}\{SINR_k^\diamond\})$$

$$\mathrm{s.t.} \quad \sum_{k=1}^{K}\mathrm{tr}\{\mathbf{Q}_k\mathbf{A}_n\} \leq P_n, \quad n \in \{1, \ldots, N\};$$

$$\mathrm{rank}\{\mathbf{Q}_k\} = 1, \quad k \in \{1, \ldots, K\}. \tag{13}$$

Suppose that $\mathbf{Q}_k = \mathbf{q}_k\mathbf{q}_k^{\mathrm{H}}$ is the solution to problem (13), then the beamforming vector for UE k becomes

$$\mathbf{w}_k = \mathbf{q}_k. \tag{14}$$

In order to find the globally optimal solution for problem (13), we resort to the polyblock algorithm [21].

B. An Upper-Bound for Each UE's Expected Rate

To apply the polyblock algorithm [21], we need to find an upper-bound for each UE's expected rate as an initialization step in the polyblock algorithm (see Appendix I for details on $\hat{\mathbf{r}}^{\mathrm{max}}$). Our results are presented in Theorem 1.

Theorem 1: UE k's expected rate is upper bounded by

$$\mathbb{E}\{\log_2(1 + SINR_k^\diamond)\} \leq \log_2(1 + \mathbb{E}\{SINR_k^\diamond\}) \leq \tilde{r}_k^{\mathrm{max}}, \tag{15}$$

where $\tilde{r}_k^{\mathrm{max}} = \log_2(1 + ((A_k^{\mathrm{ave}}P(1 - 2^B\beta(2^B, (N/(N-1)))))))/N_0)$ and $\beta(x, y)$ is the beta function defined as $\beta(x, y) = (\Gamma(x)\Gamma(y))/(\Gamma(x+y))$, where $\Gamma(\cdot)$ denotes the gamma function [28].

Proof: See Appendix II. ∎

C. Construction of the Feasibility Test

For the polyblock algorithm to work, a feasibility test should be constructed to check whether a proposed UE rate-tuple is achievable [21] (see Appendix I for details). Considering an arbitrary rate-tuple $\tilde{\mathbf{r}} = (\tilde{r}_1, \tilde{r}_2, \ldots, \tilde{r}_K)$, based on problem (13) we construct the feasibility problem required in the polyblock algorithm as

$$\mathrm{find} \quad \mathbf{Q}_k \in \mathbb{H}_N^+, \quad k \in \{1, \ldots, K\}$$

$$\mathrm{s.t.} \quad \log_2(1 + \mathbb{E}\{SINR_k^\diamond\}) \geq \tilde{r}_k, \quad k \in \{1, \ldots, K\};$$

$$\sum_{k=1}^{K}\mathrm{tr}\{\mathbf{Q}_k\mathbf{A}_n\} \leq P_n, \quad n \in \{1, \ldots, N\};$$

$$\mathrm{rank}\{\mathbf{Q}_k\} = 1, \quad k \in \{1, \ldots, K\}. \tag{16}$$

The first set of constraints in problem (16) is hard to deal with, due to the complicated mathematical form in (10). Here, we propose to tighten the first set of constraints in problem (16) as follows,

$$
\begin{aligned}
&\log_2\left(1 + \mathbb{E}\left\{SINR_k^\diamond\right\}\right)\\
&= \log_2\left(1 + \mathbb{E}\left\{SINR_k^\diamond\right\}\right)\\
&= \log_2\left(1 + \mathbb{E}\left\{\frac{A_k^{\mathrm{ave}}\tilde{\mathbf{h}}_k^\diamond\mathbf{Q}_k\tilde{\mathbf{h}}_k^{\diamond\mathrm{H}}}{A_k^{\mathrm{ave}}\sum_{j\neq k}\tilde{\mathbf{h}}_k^\diamond\mathbf{Q}_j\tilde{\mathbf{h}}_k^{\diamond\mathrm{H}}+N_0}\right\}\right)\\
&\overset{(a)}{\geq} \log_2\left(1 + \frac{A_k^{\mathrm{ave}}\mathbb{E}\left\{\tilde{\mathbf{h}}_k^\diamond\mathbf{Q}_k\tilde{\mathbf{h}}_k^{\diamond\mathrm{H}}\right\}}{A_k^{\mathrm{ave}}\mathbb{E}\left\{\sum_{j\neq k}\tilde{\mathbf{h}}_k^\diamond\mathbf{Q}_j\tilde{\mathbf{h}}_k^{\diamond\mathrm{H}}\right\}+N_0}\right)\\
&\geq \tilde{r}_k.
\end{aligned}
\tag{17}
$$

Note that the inequality (a) in (17) comes from a non-trivial proposition, which is

$$
\begin{aligned}
&\mathbb{E}\left\{\frac{A_k^{\mathrm{ave}}\tilde{\mathbf{h}}_k^\diamond\mathbf{Q}_k\tilde{\mathbf{h}}_k^{\diamond\mathrm{H}}}{A_k^{\mathrm{ave}}\sum_{j\neq k}\tilde{\mathbf{h}}_k^\diamond\mathbf{Q}_j\tilde{\mathbf{h}}_k^{\diamond\mathrm{H}}+N_0}\right\}\\
&\geq \frac{A_k^{\mathrm{ave}}\mathbb{E}\left\{\tilde{\mathbf{h}}_k^\diamond\mathbf{Q}_k\tilde{\mathbf{h}}_k^{\diamond\mathrm{H}}\right\}}{A_k^{\mathrm{ave}}\mathbb{E}\left\{\sum_{j\neq k}\tilde{\mathbf{h}}_k^\diamond\mathbf{Q}_j\tilde{\mathbf{h}}_k^{\diamond\mathrm{H}}\right\}+N_0}.
\end{aligned}
\tag{18}
$$

The validity of (18) is explained in detail as follows. Suppose that the beamforming vector for UE k is decomposed into a general form as $\mathbf{w}_k = \sqrt{\tilde{P}_k}\tilde{\mathbf{w}}_k = \sqrt{\tilde{P}_k}(\beta_k\hat{\mathbf{h}}_k^{\mathrm{H}} + \sqrt{1-|\beta_k|^2}\mathbf{v}_k)$, where $\tilde{P}_k$ is the transmission power for UE k, $\tilde{\mathbf{w}}_k$ is UE k's normalized beamforming vector, $\mathbf{v}_k$ is a unit-norm vector orthogonal to $\hat{\mathbf{h}}_k^{\mathrm{H}}$ and β_k is a complex value satisfying $|\beta_k| \in$

$[0, 1]$ to make $\tilde{\mathbf{w}}_k$ a normalized vector. Then, from (8), we can obtain

$$
\begin{aligned}
&A_k^{\mathrm{ave}}\tilde{\mathbf{h}}_k^\diamond\mathbf{Q}_k\tilde{\mathbf{h}}_k^{\diamond\mathrm{H}}\\
&= A_k^{\mathrm{ave}}\tilde{\mathbf{h}}_k^\diamond\sqrt{\tilde{P}_k}\tilde{\mathbf{w}}_k\sqrt{\tilde{P}_k}\tilde{\mathbf{w}}_k^{\mathrm{H}}\tilde{\mathbf{h}}_k^{\diamond\mathrm{H}}\\
&= A_k^{\mathrm{ave}}\tilde{P}_k\left|\left(\sqrt{1-Z}\hat{\mathbf{h}}_k + \sqrt{Z}\mathbf{e}_k^\diamond\right)\left(\beta_k\hat{\mathbf{h}}_k^{\mathrm{H}} + \sqrt{1-|\beta_k|^2}\mathbf{v}_k\right)\right|^2\\
&= A_k^{\mathrm{ave}}\tilde{P}_k\left|\sqrt{1-Z}\beta_k + \sqrt{Z}\sqrt{1-|\beta_k|^2}\mathbf{e}_k^\diamond\mathbf{v}_k\right|^2.
\end{aligned}
\tag{19}
$$

In a similar way, we decompose $\mathbf{w}_j$ as $\mathbf{w}_j = \sqrt{\tilde{P}_j}\tilde{\mathbf{w}}_j = \sqrt{\tilde{P}_j}(\beta_j\hat{\mathbf{h}}_k^{\mathrm{H}} + \sqrt{1-|\beta_j|^2}\mathbf{v}_j)$, and we can get

$$
\begin{aligned}
&A_k^{\mathrm{ave}}\sum_{j\neq k}\tilde{\mathbf{h}}_k^\diamond\mathbf{Q}_j\tilde{\mathbf{h}}_k^{\diamond\mathrm{H}}\\
&= A_k^{\mathrm{ave}}\sum_{j\neq k}\tilde{P}_j\left|\sqrt{1-Z}\beta_j + \sqrt{Z}\sqrt{1-|\beta_j|^2}\mathbf{e}_k^\diamond\mathbf{v}_j\right|^2.
\end{aligned}
\tag{20}
$$

Note that in (19) and (20), $A_k^{\mathrm{ave}}, P_k, P_j, \beta_k$, and β_j are not random variables (RVs), while $Z, \mathbf{e}_k^\diamond, \mathbf{v}_k$, and $\mathbf{v}_j$ are treated as RVs because the considered expectation operator is with respect to $[\tilde{\mathbf{h}}_k^\diamond|\hat{\mathbf{h}}_k]$ $(k \in \{1, \ldots, K\})$. From (19) and (20), $SINR_k^\diamond$ can be derived as

$$
\begin{aligned}
&SINR_k^\diamond\\
&= \frac{A_k^{\mathrm{ave}}\tilde{\mathbf{h}}_k^\diamond\mathbf{Q}_k\tilde{\mathbf{h}}_k^{\diamond\mathrm{H}}}{A_k^{\mathrm{ave}}\sum_{j\neq k}\tilde{\mathbf{h}}_k^\diamond\mathbf{Q}_j\tilde{\mathbf{h}}_k^{\diamond\mathrm{H}}+N_0}\\
&= \frac{A_k^{\mathrm{ave}}\tilde{P}_k\left|\sqrt{1-Z}\beta_k + \sqrt{Z}\sqrt{1-|\beta_k|^2}\mathbf{e}_k^\diamond\mathbf{v}_k\right|^2}{A_k^{\mathrm{ave}}\sum_{j\neq k}\tilde{P}_j\left|\sqrt{1-Z}\beta_j + \sqrt{Z}\sqrt{1-|\beta_j|^2}\mathbf{e}_k^\diamond\mathbf{v}_j\right|^2+N_0}.
\end{aligned}
\tag{21}
$$

For a conditional Z, we can compute $\mathbb{E}\{SINR_k^\diamond|Z\}$ as in (22)–(26), shown at the bottom of the page.

$$
\begin{aligned}
\mathbb{E}\left\{SINR_k^\diamond|Z\right\} &= \mathbb{E}\left\{\left.\frac{A_k^{\mathrm{ave}}\tilde{P}_k\left|\sqrt{1-Z}\beta_k + \sqrt{Z}\sqrt{1-|\beta_k|^2}\mathbf{e}_k^\diamond\mathbf{v}_k\right|^2}{A_k^{\mathrm{ave}}\sum_{j\neq k}\tilde{P}_j\left|\sqrt{1-Z}\beta_j + \sqrt{Z}\sqrt{1-|\beta_j|^2}\mathbf{e}_k^\diamond\mathbf{v}_j\right|^2+N_0}\right|Z\right\}\\
&= \mathbb{E}\left\{\left.A_k^{\mathrm{ave}}\tilde{P}_k\left|\sqrt{1-Z}\beta_k + \sqrt{Z}\sqrt{1-|\beta_k|^2}\mathbf{e}_k^\diamond\mathbf{v}_k\right|^2\right|Z\right\}\\
&\quad\times \mathbb{E}\left\{\left.\frac{1}{A_k^{\mathrm{ave}}\sum_{j\neq k}\tilde{P}_j\left|\sqrt{1-Z}\beta_j + \sqrt{Z}\sqrt{1-|\beta_j|^2}\mathbf{e}_k^\diamond\mathbf{v}_j\right|^2+N_0}\right|Z\right\}
\end{aligned}
\tag{22}
$$

$$
\begin{aligned}
&\geq \mathbb{E}\left\{\left.A_k^{\mathrm{ave}}\tilde{P}_k\left|\sqrt{1-Z}\beta_k + \sqrt{Z}\sqrt{1-|\beta_k|^2}\mathbf{e}_k^\diamond\mathbf{v}_k\right|^2\right|Z\right\}\\
&\quad\times \frac{1}{\mathbb{E}\left\{\left.A_k^{\mathrm{ave}}\sum_{j\neq k}\tilde{P}_j\left|\sqrt{1-Z}\beta_j + \sqrt{Z}\sqrt{1-|\beta_j|^2}\mathbf{e}_k^\diamond\mathbf{v}_j\right|^2+N_0\right|Z\right\}}
\end{aligned}
\tag{23}
$$

$$
= \frac{A_k^{\mathrm{ave}}\tilde{P}_k\left[(1-Z)|\beta_k|^2 + Z\left(1-|\beta_k|^2\right)\mathbb{E}\left\{|\mathbf{e}_k^\diamond\mathbf{v}_k|^2\right\}\right]}{A_k^{\mathrm{ave}}\sum_{j\neq k}\tilde{P}_j\left[(1-Z)|\beta_j|^2 + Z\left(1-|\beta_j|^2\right)\mathbb{E}\left\{|\mathbf{e}_k^\diamond\mathbf{v}_j|^2\right\}\right]+N_0}
\tag{24}
$$

$$
= \frac{A_k^{\mathrm{ave}}\tilde{P}_k|\beta_k|^2 + ZA_k^{\mathrm{ave}}\tilde{P}_k\left(\frac{1}{N-1} - \frac{N}{N-1}|\beta_k|^2\right)}{\left(A_k^{\mathrm{ave}}\sum_{j\neq k}\tilde{P}_j|\beta_j|^2 + N_0\right) + ZA_k^{\mathrm{ave}}\sum_{j\neq k}\tilde{P}_j\left(\frac{1}{N-1} - \frac{N}{N-1}|\beta_j|^2\right)}
\tag{25}
$$

$$
\overset{\triangle}{=} \frac{a+bZ}{c+dZ}
\tag{26}
$$

In (26), we define $a = A_k^{\mathrm{ave}} \tilde{P}_k |\beta_k|^2$, $b = A_k^{\mathrm{ave}} \tilde{P}_k((1/N - 1) - (N/N - 1)|\beta_k|^2)$, $c = A_k^{\mathrm{ave}} \sum_{j \neq k} \tilde{P}_j |\beta_j|^2 + N_0$, and $d = A_k^{\mathrm{ave}} \sum_{j \neq k} \tilde{P}_j ((1/N - 1) - (N/N - 1)|\beta_j|^2)$. Equation (22) follows from the fact that $\mathbf{e}_k^\diamond \mathbf{v}_k$ are $\mathbf{e}_k^\diamond \mathbf{v}_j$ are independently distributed. Inequality (23) is obtained because $\mathbb{E}\{(1/x)\} \geq (1/\mathbb{E}\{x\})$ for $x > 0$ due to the convexity of $1/x$. Equation (24) is obtained because the phases of $\mathbf{e}_k^\diamond \mathbf{v}_k$ and $\mathbf{e}_k^\diamond \mathbf{v}_j$ are independently distributed with regard to β_k and β_j, respectively. And thus the expected product of $\mathbf{e}_k^\diamond \mathbf{v}_k$ and β_k, and that of $\mathbf{e}_k^\diamond \mathbf{v}_j$ and β_j are zero. Equation (25) is calculated according to the results in [6] that $\mathbb{E}\{|\mathbf{e}_k^\diamond \mathbf{v}_k|^2\} = \mathbb{E}\{|\mathbf{e}_k^\diamond \mathbf{v}_j|^2\} = (1/N - 1)$. Furthermore, we have $\mathbb{E}\{SINR_k^\diamond\} = \mathbb{E}_{[Z]}\{\mathbb{E}\{SINR_k^\diamond|Z\}\} = \mathbb{E}_{[Z]}\{(a + bZ)/(c + dZ)\}$. Additionally, from the definition in (26), we have

$$\mathbb{E}\left\{A_k^{\mathrm{ave}} \tilde{\mathbf{h}}_k^\diamond \mathbf{Q}_k \tilde{\mathbf{h}}_k^{\diamond\mathrm{H}}\right\} = \mathbb{E}_{[Z]}\left\{\mathbb{E}\left\{A_k^{\mathrm{ave}} \tilde{\mathbf{h}}_k^\diamond \mathbf{Q}_k \tilde{\mathbf{h}}_k^{\diamond\mathrm{H}} \middle| Z\right\}\right\}$$
$$= \mathbb{E}_{[Z]}\{a + bZ\}, \qquad (27)$$

and

$$\mathbb{E}\left\{A_k^{\mathrm{ave}} \sum_{j \neq k} \tilde{\mathbf{h}}_k^\diamond \mathbf{Q}_j \tilde{\mathbf{h}}_k^{\diamond\mathrm{H}} + N_0\right\}$$
$$= \mathbb{E}_{[Z]}\left\{\mathbb{E}\left\{A_k^{\mathrm{ave}} \sum_{j \neq k} \tilde{\mathbf{h}}_k^\diamond \mathbf{Q}_j \tilde{\mathbf{h}}_k^{\diamond\mathrm{H}} + N_0 \middle| Z\right\}\right\}$$
$$= \mathbb{E}_{[Z]}\{c + dZ\}. \qquad (28)$$

In general, there is no obvious numerical relationship between $\mathbb{E}_{[Z]}\{(a+bZ)/(c+dZ)\}$ and $(\mathbb{E}_{[Z]}\{a+bZ\})/(\mathbb{E}_{[Z]}\{c+dZ\})$ since $a + bZ/c + dZ$ is neither a convex function nor a concave one. Nevertheless, considering reasonable precoding operations in practical networks, we propose the following Lemma.

Lemma 2: If $\sum_{j \neq k} |\beta_j|^4 \leq (1/N^2) \leq |\beta_k|^4$, then $\mathbb{E}_{[Z]}\{(a+bZ)/(c+dZ)\} \geq (\mathbb{E}_{[Z]}\{a+bZ\})/(\mathbb{E}_{[Z]}\{c+dZ\})$.

Proof: See Appendix III. ∎

Based on Lemma 2, we can conclude that (17) and (18) are true if $\sum_{j \neq k} |\beta_j|^4 \leq (1/N^2) \leq |\beta_k|^4$. Note that such conditions are reasonable for practical precoding operations. On one hand, $|\beta_k|^4 \geq (1/N^2)$ indicates that the beamforming vector of UE k should be roughly aligned with $\hat{\mathbf{h}}_k$ so that the

power of the useful signal could be fairly large. On the other hand, $\sum_{j \neq k} |\beta_j|^4 \leq (1/N^2)$ implies that $|\beta_j|^2$ should be relatively small, which is the typical case in reasonable precoding schemes that the expected inter-UE interference leakage should be kept low.

From (17) and Lemma 2, we re-formulate problem (16) as

find $\quad \mathbf{Q}_k \in \mathbb{H}_N^+, \quad k \in \{1, \ldots, K\}$

s.t. $\quad \dfrac{A_k^{\mathrm{ave}} \mathbb{E}\left\{\tilde{\mathbf{h}}_k^\diamond \mathbf{Q}_k \tilde{\mathbf{h}}_k^{\diamond\mathrm{H}}\right\}}{A_k^{\mathrm{ave}} \sum_{j \neq k} \mathbb{E}\left\{\tilde{\mathbf{h}}_k^\diamond \mathbf{Q}_j \tilde{\mathbf{h}}_k^{\diamond\mathrm{H}}\right\} + N_0} \geq (2^{\tilde{r}_k} - 1);$

$$\sum_{k=1}^K \mathrm{tr}\{\mathbf{Q}_k \mathbf{A}_n\} \leq P_n, \quad n \in \{1, \ldots, N\};$$

$$\mathrm{rank}\{\mathbf{Q}_k\} = 1, \quad k \in \{1, \ldots, K\}. \qquad (29)$$

In problem (29), $\mathbb{E}\{\tilde{\mathbf{h}}_k^\diamond \mathbf{Q}_k \tilde{\mathbf{h}}_k^{\diamond\mathrm{H}}\}$ can be computed as (30), shown at the bottom of the page.

In (30), the equation (a) is obtained according to the result in [8] that $\mathbb{E}\{\mathbf{e}_k^{\diamond\mathrm{H}} \mathbf{e}_k^\diamond\} = (1/N-1)(\mathbf{I}_N - \hat{\mathbf{h}}_k^\mathrm{H} \hat{\mathbf{h}}_k)$. Besides, $\mathbf{U}_k$ is denoted as $\mathbf{U}_k = (1 - (N\mathbb{E}\{Z\}/(N-1)))\hat{\mathbf{h}}_k^\mathrm{H}\hat{\mathbf{h}}_k + (\mathbb{E}\{Z\}/(N-1))\mathbf{I}_N$, where $\mathbb{E}\{Z\}$ can be calculated using (44) and $\mathbf{U}_k$ is positive definite because of (45). From (30), we can also get $\mathbb{E}\{\tilde{\mathbf{h}}_k^\diamond \mathbf{Q}_j \tilde{\mathbf{h}}_k^{\diamond\mathrm{H}}\} = \mathrm{tr}\{\mathbf{Q}_j \mathbf{U}_k\}$. Note that unlike (19), the calculation in (30) retains the semi-definite matrix form of $\mathbf{Q}_k$, which is required in solving SDP problems such as problem (29).

D. Transformation of the Feasibility Test

Apparently problem (29) is non-convex due to the rank-one constraints. Here, we apply the SDP relaxation [29] by dropping the rank-one constraints on $\{\mathbf{Q}_k\}$ and transform it into a convex one shown as

find $\quad \mathbf{Q}_k \in \mathbb{H}_N^+, \quad k \in \{1, \ldots, K\}$

s.t. $\quad A_k^{\mathrm{ave}} \mathrm{tr}\{\mathbf{Q}_k \mathbf{U}_k\} \geq (2^{\tilde{r}_k} - 1)\left(A_k^{\mathrm{ave}} \sum_{j \neq k} \mathrm{tr}\{\mathbf{Q}_j \mathbf{U}_k\} + N_0\right);$

$$\sum_{k=1}^K \mathrm{tr}\{\mathbf{Q}_k \mathbf{A}_n\} \leq P_n, \quad n \in \{1, \ldots, N\}. \qquad (31)$$

$$\mathbb{E}\left\{\tilde{\mathbf{h}}_k^\diamond \mathbf{Q}_k \tilde{\mathbf{h}}_k^{\diamond\mathrm{H}}\right\} = \mathbb{E}\left\{\mathrm{tr}\left\{\mathbf{Q}_k \left(\tilde{\mathbf{h}}_k^{\diamond\mathrm{H}} \tilde{\mathbf{h}}_k^\diamond\right)\right\}\right\}$$
$$= \mathbb{E}\left\{\mathrm{tr}\left\{\mathbf{Q}_k \left[\left(\sqrt{1-Z}\hat{\mathbf{h}}_k + \sqrt{Z}\mathbf{e}_k^\diamond\right)^\mathrm{H} \left(\sqrt{1-Z}\hat{\mathbf{h}}_k + \sqrt{Z}\mathbf{e}_k^\diamond\right)\right]\right\}\right\}$$
$$= \mathrm{tr}\left\{\mathbf{Q}_k \left(\mathbb{E}\{1-Z\}\hat{\mathbf{h}}_k^\mathrm{H}\hat{\mathbf{h}}_k + \mathbb{E}\{Z\}\mathbb{E}\{\mathbf{e}_k^{\diamond\mathrm{H}}\mathbf{e}_k^\diamond\}\right)\right\}$$
$$\overset{(a)}{=} \mathrm{tr}\left\{\mathbf{Q}_k \left[(1 - \mathbb{E}\{Z\})\hat{\mathbf{h}}_k^\mathrm{H}\hat{\mathbf{h}}_k + \frac{\mathbb{E}\{Z\}}{N-1}\left(\mathbf{I}_N - \hat{\mathbf{h}}_k^\mathrm{H}\hat{\mathbf{h}}_k\right)\right]\right\}$$
$$= \mathrm{tr}\left\{\mathbf{Q}_k \left[\left(1 - \frac{N\mathbb{E}\{Z\}}{N-1}\right)\hat{\mathbf{h}}_k^\mathrm{H}\hat{\mathbf{h}}_k + \frac{\mathbb{E}\{Z\}}{N-1}\mathbf{I}_N\right]\right\}$$
$$= \mathrm{tr}\{\mathbf{Q}_k \mathbf{U}_k\} \qquad (30)$$

It should be noted that although problem (31) exhibits similar forms compared with a previously treated problem in [30], which is shown in (41) (see Appendix I for more details), the statement for problem (41) that the optimization problem always has a solution of rank-one matrices [30] does not hold for problem (31). The detailed reason is explained as follows.

According to [30], for any solution of problem (41) containing a certain matrix $\mathbf{Q}_k^*$ with rank higher than one, $\mathbf{Q}_k^*$ can be replaced by an alternative matrix $\mathbf{Q}_k^{**}$, which is the solution to the sub-problem expressed as

$$\max_{\mathbf{Q}_k \in \mathbb{H}_N^+} \quad \check{\mathbf{h}}_k \mathbf{Q}_k \check{\mathbf{h}}_k^{\mathrm{H}}$$
$$\text{s.t.} \quad \mathrm{tr}\left\{\mathbf{Q}_k \check{\mathbf{h}}_j^{\mathrm{H}} \check{\mathbf{h}}_j\right\} \leq \mathrm{tr}\left\{\mathbf{Q}_k^* \check{\mathbf{h}}_j^{\mathrm{H}} \check{\mathbf{h}}_j\right\}, \; j \neq k;$$
$$\mathrm{tr}\{\mathbf{Q}_k \mathbf{A}_n\} \leq \mathrm{tr}\{\mathbf{Q}_k^* \mathbf{A}_n\}. \quad (32)$$

Problem (32) tries to maximize the signal power of UE k with neither more inter-UE interference nor more per-antenna power consumption than those of $\mathbf{Q}_k^*$. Thus, the solution $\mathbf{Q}_k^{**}$ to problem (32) is also a solution to problem (41) because $\mathbf{Q}_k^{**}$ is feasible and no worse than $\mathbf{Q}_k^*$ for problem (41). Furthermore, Lemma 1 of [25] guarantees that $\mathbf{Q}_k^{**}$ is always rank-one, and hence $\mathbf{Q}_k^{**}$ is also the solution to the original feasibility problem (40). However, in problem (31), $\mathrm{tr}\{\mathbf{Q}_k \mathbf{U}_k\}$ cannot be written in a quadratic form such as $\check{\mathbf{h}}_k \mathbf{Q}_k \check{\mathbf{h}}_k^{\mathrm{H}}$, so that the method to find an alternative solution of rank-one matrices based on Lemma 1 of [25] does not work here. Therefore, the transformed problem (31) is not equivalent to the feasibility problem (29). To make the solution of problem (31) valid for problem (29), we need to extract an approximate solution of rank-one matrices from that of problem (31). An effective way to perform the task is the randomization technique, which interprets an SDP problem as a stochastic quadratically constrained quadratic program (QCQP) problem [31]. However, it is not easy to simultaneously draw K rank-one beamforming matrices from the solution of problem (31) because all $\mathbf{Q}_k$s are intertwined in the constraints. Hence, in order to efficiently apply the randomization technique, similar to problem (32), we also propose an SDP sub-problem represented as

$$\max_{\mathbf{Q}_k \in \mathbb{H}_N^+} \quad \mathrm{tr}\{\mathbf{Q}_k \mathbf{U}_k\}$$
$$\text{s.t.} \quad \mathrm{tr}\{\mathbf{Q}_k \mathbf{U}_j\} \leq \mathrm{tr}\left\{\tilde{\mathbf{Q}}_k^* \mathbf{U}_j\right\}, \; j \neq k;$$
$$\mathrm{tr}\{\mathbf{Q}_k \mathbf{A}_n\} \leq \mathrm{tr}\left\{\tilde{\mathbf{Q}}_k^* \mathbf{A}_n\right\}, \quad (33)$$

where $\{\tilde{\mathbf{Q}}_k^*\}$, possibly containing multi-rank matrices, is the solution to problem (31). The purpose of introducing problem (33) is to find an alternative solution with rank-one matrices for problem (31) in a decoupled way, i.e., only a single $\mathbf{Q}_k$ is treated in problem (33), so that the randomization technique can be applied on a per-UE basis. Like problem (32), problem (33) also aims at maximizing the useful signal of UE k with neither more inter-UE interference nor more per-antenna power consumption than $\tilde{\mathbf{Q}}_k^*$. Therefore, as long as the transformed feasibility problem (31) has a solution $\tilde{\mathbf{Q}}_k^*$, problem (33) can generate another solution for problem (31) denoted as $\tilde{\mathbf{Q}}_k^{**}$ to supersede $\tilde{\mathbf{Q}}_k^*$.

E. Solution of the Feasibility Test

It should be noted that in [32], the authors proved that the solution of an SDP problem such as problem (33) is rank-one only if it has at most three constraints. However, problem (33) has $N + K - 1$ constraints, which is in general larger than three. Therefore, we consider the randomization technique [31] to find the rank-one matrix solution for problem (33). Suppose that $\tilde{\mathbf{Q}}_k^{**}$ is a matrix with rank higher than one. Then according to [31], we can generate a random vector $\tilde{\mathbf{q}}_k \sim \mathcal{N}(\mathbf{0}, \tilde{\mathbf{Q}}_k^{**})$ and scale it by a factor ρ to ensure no violation of the constraints in problem (33), i.e.,

$$\mathbf{q}_k = \rho \tilde{\mathbf{q}}_k, \quad (34)$$

where ρ can be computed as

$$\rho = \min_{j,n} \left(\sqrt{\frac{\mathrm{tr}\left\{\tilde{\mathbf{Q}}_k^* \mathbf{U}_j\right\}_{j \neq k}}{\mathrm{tr}\left\{\tilde{\mathbf{q}}_k \tilde{\mathbf{q}}_k^{\mathrm{H}} \mathbf{U}_j\right\}_{j \neq k}}}, \sqrt{\frac{\mathrm{tr}\left\{\tilde{\mathbf{Q}}_k^* \mathbf{A}_n\right\}}{\mathrm{tr}\left\{\tilde{\mathbf{q}}_k \tilde{\mathbf{q}}_k^{\mathrm{H}} \mathbf{A}_n\right\}}} \right). \quad (35)$$

Now $\mathbf{q}_k \mathbf{q}_k^{\mathrm{H}}$ becomes an approximate rank-one matrix solution for the feasibility problem (29). The vector randomization process is repeated by L_{rand} times and we select the vector that gives the largest performance measure for problem (33) as a final solution, i.e.,

$$\mathbf{q}_k^{**} = \arg\max_{\mathbf{q}_k^{(i)}, i \in \{1, 2, \ldots, L_{\mathrm{rand}}\}} \left(\mathrm{tr}\left\{\mathbf{q}_k^{(i)} \mathbf{q}_k^{(i)\mathrm{H}} \mathbf{U}_k\right\} \right). \quad (36)$$

According to [31], the extracted rank-one solution is in general a good approximation of the original solution as long as L_{rand} is sufficiently large.

F. Algorithm Summary

With the problem (16) for feasibility test in the polyblock algorithm being re-formulated as problem (29), then being transformed into problem (31), and finally being solved in problem (33) by means of the randomization technique, we can summarize the proposed scheme in Algorithm 1, which will be referred to as the robust beamforming based on the polyblock algorithm with per-antenna power constraints (shorten as the RPb-PA scheme in the sequel). An important note on the core part of Algorithm 1, i.e., finding the solution to problem (33), is that it implies a robust design of precoding. To be more specific, in the first set of constraints in problem (33), let us denote $\tilde{\gamma}_{k,j} = \mathrm{tr}\{\tilde{\mathbf{Q}}_k^* \mathbf{U}_j\}$ and decompose $\tilde{\gamma}_{k,j}$ as $\tilde{\gamma}_{k,j} = \gamma_{k,j} p_{\mathrm{leak}}$, where p_{leak} and $\gamma_{k,j}$ will later be respectively interpreted as a certain probability of inter-UE interference leakage (e.g., 90%) and a leakage threshold for interference from UE k to UE j. We can rewrite the first set of constraints in problem (33) as

$$\mathrm{tr}\{\mathbf{Q}_k \mathbf{U}_j\} \leq \gamma_{k,j} p_{\mathrm{leak}}, \quad j \in \{1, \ldots, K\} \text{ and } j \neq k. \quad (37)$$

According to Proposition 1 in [11], (37) is a sufficient condition for the following guaranteed performance of interference leakage,

$$\Pr\{\mathbf{w}_k^{\mathrm{H}} \mathbf{U}_j \mathbf{w}_k \geq \gamma_{k,j}\} \leq p_{\mathrm{leak}}, \quad j \in \{1, \ldots, K\} \text{ and } j \neq k. \quad (38)$$

Now in (38), p_{leak} is a given probability (e.g., 90%) of the concerned large leakage event expressed in mathematics as $\mathbf{w}_k^{\text{H}} \mathbf{U}_j \mathbf{w}_k \geq \gamma_{k,j}$. As a result, problem (33) implicitly provides a probabilistic guarantee that the resulting interference leakage of our design is below a certain level by a given probability. Note that (38) still holds when $\tilde{\mathbf{Q}}_k^*$ is rank-one. Thus, the robustness of the proposed scheme always exists.

Algorithm 1 The proposed RPb-PA scheme

Step 1: Initialization
  • Compute $\tilde{\mathbf{r}}^{\text{max}} = (\tilde{r}_1^{\text{max}}, \tilde{r}_2^{\text{max}}, \ldots, \tilde{r}_K^{\text{max}})$ using (15) in Theorem 1.
  • Construct the set containing the outer boundary rate-tuples: $\mathcal{V}^{(1)} = \{\tilde{\mathbf{r}}^{\text{max}}\}$.
  • Set the feasible rate-tuple $\tilde{\mathbf{r}}^{\text{inner}} = \mathbf{0}$ and $l = 1$.
Step 2: Iteration
  • $\tilde{\mathbf{r}}^{\text{outer}} = \arg\max\{g(\tilde{\mathbf{r}}) | \tilde{\mathbf{r}} \in \mathcal{V}^{(l)}\}$.
  • Find the intersection point of the boundary of the achievable rate region with the segment between $\mathbf{0}$ and $\tilde{\mathbf{r}}^{\text{outer}}$ by the bisection method. The problem is formulated as follows and its solution is denoted as t^{opt}.

$$\max \quad t \in [0, 1)$$

$$\text{s.t.} \quad \text{Problem (31) is feasible with } t\tilde{\mathbf{r}}^{\text{outer}}.$$

  • $\tilde{\mathbf{r}}^{(l)} = t^{\text{opt}} \tilde{\mathbf{r}}^{\text{outer}}$ and $\tilde{\mathbf{r}}^{\text{inner}} = \arg\max\{g(\tilde{\mathbf{r}}^{\text{inner}}), g(\tilde{\mathbf{r}}^{(l)})\}$.
  • If $g(\tilde{\mathbf{r}}^{\text{inner}}) + \varepsilon \geq g(\tilde{\mathbf{r}}^{\text{outer}})$, terminate the iteration and go to Step 4;
    Else, update $\mathcal{V}^{(l+1)}$ as $\mathcal{V}^{(l+1)} = (\mathcal{V}^{(l)} \setminus \{\tilde{\mathbf{r}}^{\text{outer}}\}) \cup \{\tilde{\mathbf{r}}^{\text{outer},k} | k = 1, 2, \ldots, K\}$, where $\tilde{\mathbf{r}}^{\text{outer},k} = (\tilde{r}_1^{\text{outer}}, \tilde{r}_2^{\text{outer}}, \ldots, \tilde{r}_k^{\text{inner}}, \ldots, \tilde{r}_K^{\text{outer}})$. Then eliminate the rate-tuples in $\mathcal{V}^{(l+1)}$ that are not Pareto optimal, i.e., $\forall \tilde{\mathbf{r}}$ satisfying $\{\tilde{\mathbf{r}} \leq \tilde{\mathbf{r}}' | \tilde{\mathbf{r}}, \tilde{\mathbf{r}}' \in \mathcal{V}^{(l+1)}, \tilde{\mathbf{r}} \neq \tilde{\mathbf{r}}'\}$.
Step 3: Termination
  • $l = L_{\text{max}}$, where L_{max} is the maximum iteration number. Go to Step 4;
    Else, $l = l + 1$, return to Step 2.
Step 4: Output
  • Solve problem (31) on condition of $\tilde{\mathbf{r}}^{\text{inner}}$ and obtain the solution $\{\tilde{\mathbf{Q}}_k^*\}$.
  • For each $\tilde{\mathbf{Q}}_k^*$ that is not rank-one, solve problem (33) on condition of $\tilde{\mathbf{Q}}_k^*$ and obtain its solution $\tilde{\mathbf{Q}}_k^{**}$. For other $\tilde{\mathbf{Q}}_k^*$, set $\tilde{\mathbf{Q}}_k^{**} = \tilde{\mathbf{Q}}_k^*$.
  • For each $\tilde{\mathbf{Q}}_k^{**}$ that is not rank-one, use (34)–(36) to obtain $\mathbf{q}_k^{**}$ and set $\tilde{\mathbf{Q}}_k^{***} = \mathbf{q}_k^{**} \mathbf{q}_k^{**\text{H}}$. For other $\tilde{\mathbf{Q}}_k^{**}$, set $\tilde{\mathbf{Q}}_k^{***} = \tilde{\mathbf{Q}}_k^{**}$.
  • Output $\tilde{\mathbf{Q}}_k^{***}$ as the solution to problem (13) and get UEs' beamforming vectors according to (14).

In Algorithm 1, Step 2 refines the outer boundary rate-tuple $\tilde{\mathbf{r}}^{\text{outer}}$ to a inner feasible rate tuple $\tilde{\mathbf{r}}^{\text{inner}}$ in the polyblock algorithm [21] using the bisection search, which is operated by iteratively checking whether problem (31) is feasible with an updated t for L_{bi} times, resulting in a numerical precision of $1/2^{L_{\text{bi}}}$ for t. The boundary refinery process is stopped when

$g(\tilde{\mathbf{r}}^{\text{outer}})$ converges to $g(\tilde{\mathbf{r}}^{\text{inner}})$ with a gap of ε. As explained earlier, it should be noted that in some very recent works [11], [12], the authors directly proposed an optimization problem, which bears some similarity to our problem (33), from the perspective of probabilistic leakage control that $\text{tr}\{\mathbf{Q}_k \mathbf{U}_j\}$ can be interpreted as interference leakage form UE k to j. The problem in [11] and [12] is described as

$$\max_{\mathbf{Q}_k \in \mathbb{H}_N^+} \quad \text{tr}\{\mathbf{Q}_k \mathbf{U}_k\}$$

$$\text{s.t.} \quad \sum_{j=1, j \neq k}^{K} \text{tr}\{\mathbf{Q}_k \mathbf{U}_j\} \leq p_{\text{leak}} \gamma_k;$$

$$\text{tr}\{\mathbf{Q}_k\} \leq \tilde{P}_k, \tag{39}$$

where p_{leak} is a given probability of the event that the expected leakage power exceeds a threshold γ_k. Considering that there are only two constraints in problem (39), its solution is always a rank-one matrix [32]. In the following, the robust beamforming scheme based on problem (39) will be referred to as the probabilistic leakage control (PLC) scheme. As opposed to the proposed accurate per-UE-pair leakage control based on $\tilde{\mathbf{Q}}_k^*$ in problem (33), a rough constraint on the sum of the expected leakage power from UE k to the other UEs is applied in problem (39) of the PLC scheme. Besides, per-UE power constraints are considered in problem (39) while we adopt a more realistic per-antenna power constraints in problem (33). It should be noted that the parameters p_{leak} and γ_k are determined using empirical methods in [11] and [12], which cannot guarantee a good performance for each channel realization. On the other hand, $\tilde{\mathbf{Q}}_k^*$ in our problem (33) is derived iteratively based on the polyblock algorithm, which is able to well exploit the available CDI and thus the proposed RPb-PA scheme should deliver a better performance than the PLC scheme. However, the RPb-PA scheme apparently involves much more computational complexity compared with the PLC scheme. In the next section, we will show the performance and complexity of the interested schemes by means of computer simulations.

V. SIMULATION RESULTS AND DISCUSSIONS

In this section, we present simulation results to compare the average weighted sum-rate performance of the ZF-PA, NROpt-PA, PLC and the proposed RPb-PA schemes. The simulation parameters are configured as $(N, K) = (4, 4)$, $[\alpha_1, \alpha_2, \alpha_3, \alpha_4] = [2, 2, 1, 1]$, $P_k = (P/N)$ and the number of CDI feedback bits $B = 4, 8, 12,$ or 16. For the PLC scheme, γ_k and p_{leak} are respectively set to 0.9 and 0.05 as in [12]. Besides, equal power allocation among UEs, i.e., $\tilde{P}_k = (P/K)$, which may violate the per-antenna constraints, is employed for the PLC scheme because that the power allocation issue was not treated in [11] or [12]. In the NROpt-PA and the proposed RPb-PA schemes, $L_{\text{bi}} = 7$, $\varepsilon = 0.1$, and $L_{\text{max}} = 100$. In addition, for the randomization technique in the RPb-PA scheme, $L_{\text{rand}} = 1000$. Moreover, we define the BS's SNR as $SNR = P/N_0$. All channels are assumed to experience uncorrelated Rayleigh fading and the entries of $\mathbf{h}_k$ are i.i.d. ZMCSCG random variables with unit variance. The results are averaged over 10 000 independent channel realizations.
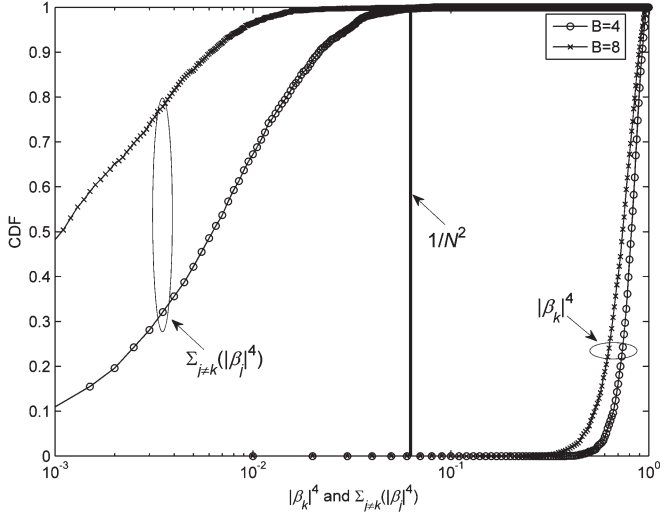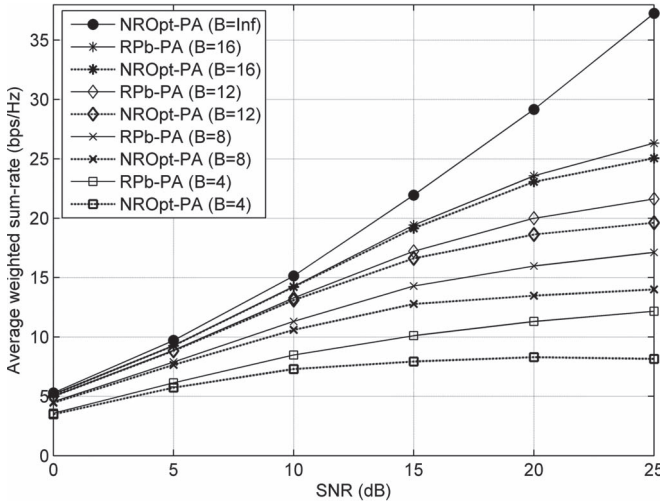
Fig. 2.   Verification of the conditions of Lemma 2.

Fig. 4.   Average weighted sum-rate of the RPb-PA scheme with perfect and average CMI for various B.

Fig. 3.   Asymptotic average weighted sum-rate with various B and perfect CMI.

A. Verification of the Conditions of Lemma 2

First, we need to verify the conditions of Lemma 2 so that the transformation of problem (16) into problem (29) is valid for the proposed RPb-PA scheme. The cumulative density functions (CDFs) of $|\beta_k|^4$ and $\sum_{j \neq k} |\beta_j|^4$ when $SNR = 10$ dB are plotted in Fig. 2. As can be seen from Fig. 2, the probability that $|\beta_k|^4 \geq (1/N^2)$ (the first condition of Lemma 2) is very high in the proposed precoding scheme, which ensures good reception quality of the useful signals. Moreover, the second condition of Lemma 2 is also verified by showing that $\sum_{j \neq k} |\beta_j|^4 \leq (1/N^2)$ is true with a high probability in Fig. 2.

B. Asymptotic Performance of the Proposed Scheme

In Fig. 3, we investigate the average weighted sum-rate performance of the NROpt-PA and RPb-PA schemes with various B under perfect CMI. Here, perfect CMI means that A_k^{ave} is replaced with $\|\mathbf{h}_k\|^2$ in the corresponding formulae throughout this paper. It is safe to state that when B goes to infinity, the average weighted sum-rate of the considered system should attain its maximum value using the NROpt-PA scheme, since
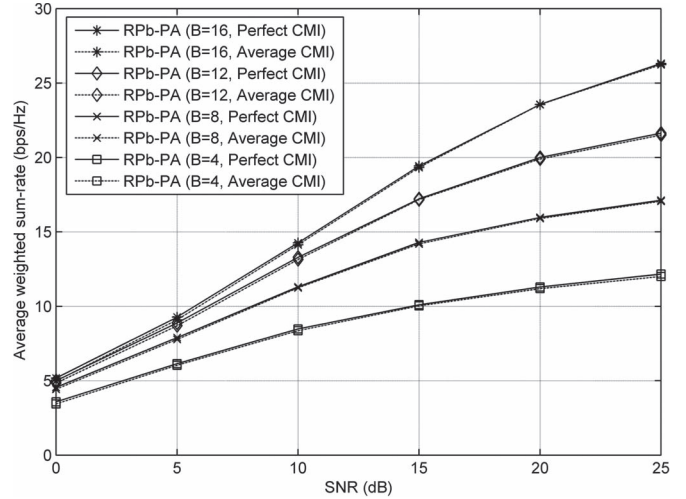
it is theoretically optimal in the case of perfect CSI. As can be observed from Fig. 3, the NROpt-PA scheme with infinite B indeed gives the performance upper-bound and the performance of the proposed RPb-PA scheme approaches the upper-bound very quickly as B increases. In particular, when $B = 16$ and $SNR = 10$ dB, the performance gap between the proposed RPb-PA scheme and the NROpt-PA scheme with $B = \infty$ is less than 1 bps/Hz, which shows superior performance of the proposed scheme. It should be noted that when B becomes larger the performance gain offered by the proposed RPb-PA scheme over the NROpt-PA scheme reduces. This is because that the channel uncertainties gradually diminish as B increases, so that when B is sufficiently large, the expectation operation will lose its purpose in problem (13), which will then degenerate to problem (7) of the NROpt-PA scheme.

C. Impact of Imperfect CMI

To study the impact of imperfect CMI on the system performance, in Fig. 4 we show the average weighted sum-rate of the RPb-PA scheme with both average and perfect CMI for $B = 4$, 8, 12, or 16. For the case of average CMI, we have $A_k^{\mathrm{ave}} = N$ because that for Rayleigh fading channels $\|\mathbf{h}_k\|^2$ is chi-square distributed with $2N$ degrees of freedom and its mean is N [33]. From Fig. 4, we can find that the performance with perfect CMI and that with average CMI are almost the same, indicating minor effectiveness of quantizing the CMI on the system performance. Note that similar results have also been reported in the design of feedback-bit partitioning for cooperative multicell systems [16], in which the authors proposed that one bit of CMI feedback is sufficient to achieve the data rates that are very close to the results of the perfect CMI case.

It should be noted that the values of α_k's may have an impact on the system with imperfect CMI. In Fig. 5, we conduct a simulation with $[\alpha_1, \alpha_2, \alpha_3, \alpha_4] = [1, 1, 1, 1]$. As can be observed from Fig. 5, when B and the difference of α_k's are small, the importance of having accurate CMI is more manifest, especially in low SNR regime. This observation is not surprising because an MU system with equally important UEs is tend to fully
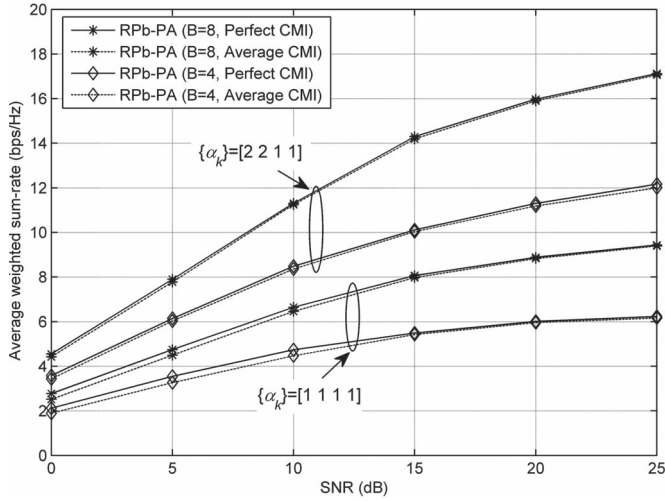
Fig. 5.   Average weighted sum-rate of the RPb-PA scheme with perfect and average CMI for different α_ks.
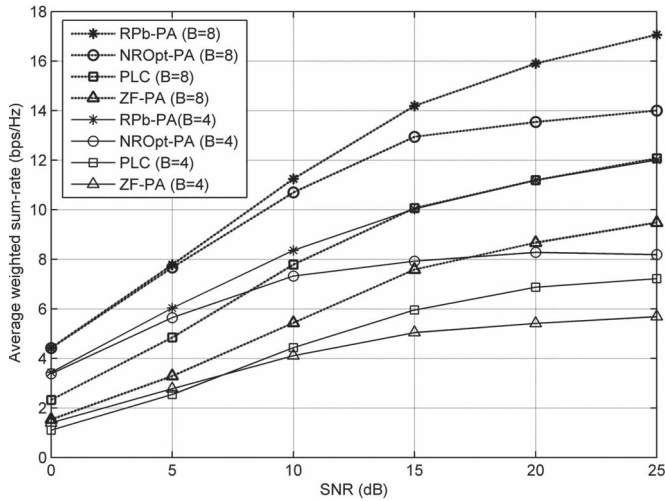

Fig. 6.   Average weighted sum-rate of the interested schemes with average CMI.

occupy all the available spatial domain resources, and thus requires more precise CDI and CMI. In addition, when the noise dominates the MU communication (low SNR regime) and the CDI is less accurate, CMI with good precision is beneficial for the BS to perform smart power loading among UEs. Nevertheless, the largest performance gap between the results of perfect CMI and those of average CMI is less than 0.4 bps/Hz. In general, it has been shown that average CMI is sufficient for the considered system to achieve a satisfactory performance close to that of perfect CMI. Hence, in the following simulations, we only consider the practical case of average CMI.

D. Comparison of Average Weighted Sum-Rate Performance

In Fig. 6, we show the average weighted sum-rate performance of the interested schemes when $B = 4, 8$ in the case of average CMI. As can be seen from Fig. 6, the proposed RPb-PA scheme exhibits substantial performance gains compared with other schemes, especially in high SNR regime, because the formulated problem (13) directly maximizes an upper-bound for the expected weighted sum-rate, leading to a superior
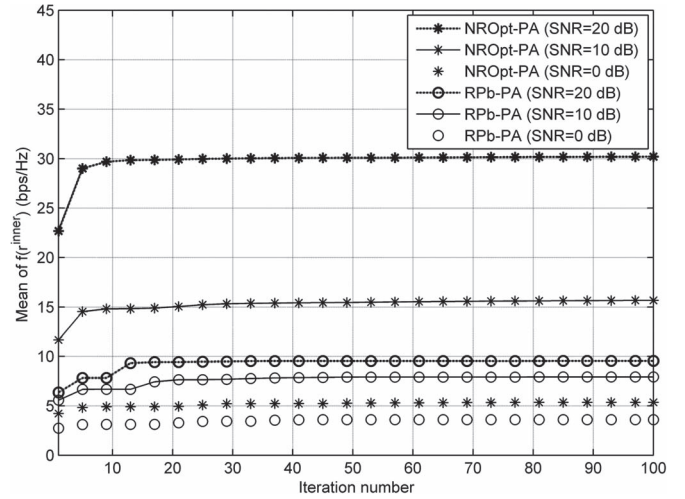

Fig. 7.   Convergence of the NROpt-PA and RPb-PA schemes with average CMI.

performance. Although the PLC scheme achieves a higher weighted sum-rate than the ZF-PA scheme, its performance is still poorer than that of the NROpt-PA scheme because of its indirect approach to maximize the weighted sum-rate. As for the NROpt-PA scheme, its computational complexity is nearly the same as that of the proposed RPb-PA scheme. However, due to CDI quantization errors, its performance curves stop increasing when the SNR is moderately large. Similar observation can also be drawn for those curves of the ZF-PA scheme, which stresses the importance of considering the channel uncertainties in system design when dealing with quantized CDI. In particular, the non-robust NROpt-PA scheme with $B = 4$ shows a slightly worse performance when $SNR = 25$ dB compared with that of $SNR = 20$ dB; whereas, the robust RPb-PA scheme shows better and more stable performance in high SNR regime. This is because that, in a robust beamforming design the channel uncertainties are considered beforehand, and hence its performance will be better than that of the non-robust design especially when channel distortions dominate the performance, e.g., in high SNR regime.

E. Algorithm Convergence Behavior

To address the convergence behavior of the NROpt-PA and RPb-PA schemes, we plot the mean of $g(\tilde{\mathbf{r}}^{\text{inner}})$ versus the iteration number l in Fig. 7 under average CMI when $B = 4$ and $SNR = 0, 10, 20$ dB. As can be seen from Fig. 7, the NROpt-PA and RPb-PA schemes need at least 15 iterations to output the final solutions, which is relatively slow. Hence, the complexity of either scheme is significantly higher than that of the PLC or ZF-PA scheme, which requires no iterative computation at all. An interesting observation from Fig. 7 is that the NROpt-PA scheme exhibits much higher performance of $g(\tilde{\mathbf{r}}^{\text{inner}})$ than the proposed RPb-PA scheme, while such advantage is not reflected in the performance comparison of the average weighted sum-rate. The reason is that $g(\tilde{\mathbf{r}}^{\text{inner}})$ is merely a BS's estimation on the weighted sum-rate, and unlike the RPb-PA scheme, the NROpt-PA scheme is prone to over-estimate the achievable data rates since it ignores the fact that CDI quantization errors may inflict serious inter-UE interference to the considered system.

F. Complexity Analysis

Regarding the comparison of computational complexity between the proposed RPb-PA scheme and the existing schemes, e.g., the PLC scheme, the most time-consuming part of the proposed scheme is Step 2 in Algorithm 1, i.e., refining the outer boundary of the feasible region by finding an appropriate parameter t using the bisection method that requires checking the feasibility of problem (31) for $L_{bi} = 7$ times in our simulations. Considering that the complexity of solving problem (31) is comparable to that of solving problem (39), the complexity of performing one iteration in Algorithm 1 is roughly seven times as much as that of the PLC scheme. Furthermore, Fig. 7 shows that the proposed RPb-PA algorithm at least entails 15 iterations for its convergence, and hence the complexity of the proposed RPb-PA algorithm is immensely higher than the PLC scheme by at least $7 \times 15 = 105$ times, making it very difficult to be applied in practice. However, the goal of this paper is to improve the sum-rate performance by allowing more complexity, which is the initial stage to find the beamforming scheme with superior performance. And the next stage is to find a low-complexity algorithm with a reasonable tradeoff between performance and complexity. Nevertheless, the proposed RPb-PA scheme stands as a good benchmark for robust beamforming designs.

As future works, low-complexity implementations, the impact of CDI feedback delay, as well as more practical fading channel models and non-RVQ CDI codebooks will be considered for the proposed beamforming schemes. In addition, extensions to more general system models such as MIMO relay networks [34], multi-cell cooperative broadcast channels [35] and Adhoc networks [36], [37] are worth to be investigated.

VI. Conclusion

In this paper, robust beamforming for MU-MISO system with per-antenna power constraints and quantized CDI is studied. Based on the polyblock algorithm, we propose a robust beamforming scheme, i.e., the RPb-PA scheme. Simulation results show that the proposed RPb-PA scheme can achieve much better performance than the existing schemes in terms of the average weighted sum-rate performance, especially when the SNR is high. The impact of imperfect CMI, the algorithm convergence behavior, the complexity issue as well as the asymptotic performance with a large number of CDI quantization bits are also discussed for the proposed scheme.

APPENDIX I
DETAILS OF THE POLYBLOCK ALGORITHM [21]

As an initialization step of the polyblock algorithm, an upper-bound rate-tuple should be found as the starting point of the refinery process of the feasible rate region [21]. More specifically, for UE k, when the BS employs the maximum ratio combining (MRC) beamforming, i.e., $\mathbf{w}_k^{MRC} = \sqrt{P}\hat{\mathbf{h}}_k^H$, and mutes the transmissions of the other $K - 1$ UEs, i.e., $\mathbf{w}_j = \mathbf{0}$, $j \in \{1, \dots, K\}$ and $j \neq k$, $\hat{r}_k$ can achieve its maximum value expressed as $\hat{r}_k^{max} = \log_2(1 + (A_k^{ave}P/N_0))$. From

$\{\hat{r}_k^{max}\}$, we can obtain an upper-bound rate-tuple as $\hat{\mathbf{r}}^{max} = (\hat{r}_1^{max}, \hat{r}_2^{max}, \dots, \hat{r}_K^{max})$. Obviously, for any achievable UE rate-tuple $\hat{\mathbf{r}} = (\hat{r}_1, \hat{r}_2, \dots, \hat{r}_K)$, it follows that $\hat{\mathbf{r}} \leq \hat{\mathbf{r}}^{max}$ and $g(\hat{\mathbf{r}}) \leq g(\hat{\mathbf{r}}^{max})$, where $g(\hat{\mathbf{r}})$ is defined as $g(\hat{\mathbf{r}}) = \sum_{k=1}^{K} \alpha_k \hat{r}_k$.

The prerequisite for applying the polyblock algorithm on problem (7) is to create a feasibility problem to test whether a certain UE rate-tuple $(\hat{r}_1, \hat{r}_2, \dots, \hat{r}_K)$ is achievable [21]. Here, the feasibility problem can be constructed according to the original problem (7) as

$$
\begin{aligned}
\text{find} \quad & \mathbf{Q}_k \in \mathbb{H}_N^+, \quad k \in \{1, \dots, K\} \\
\text{s.t.} \quad & \log_2 \left(1 + \frac{\check{\mathbf{h}}_k \mathbf{Q}_k \check{\mathbf{h}}_k^H}{\sum_{j \neq k} \check{\mathbf{h}}_k \mathbf{Q}_j \check{\mathbf{h}}_k^H + N_0} \right) \geq \hat{r}_k; \\
& \sum_{k=1}^{K} \text{tr}\{\mathbf{Q}_k \mathbf{A}_n\} \leq P_n; \\
& \text{rank}\{\mathbf{Q}_k\} = 1. \quad (40)
\end{aligned}
$$

Recently, the authors of [30] proved that the rank-one constraints in a optimization problem like the one given by (40) are redundant as long as the problem is feasible. Therefore, we can ignore the rank-one constraints on $\{\mathbf{Q}_k\}$ and transform the feasibility problem (40) into a convex one with constraints of affine transformation of second-order cones [29] shown as

$$
\begin{aligned}
\text{find} \quad & \mathbf{Q}_k \in \mathbb{H}_N^+, \quad k \in \{1, \dots, K\} \\
\text{s.t.} \quad & \check{\mathbf{h}}_k \mathbf{Q}_k \check{\mathbf{h}}_k^H \geq (2^{\hat{r}_k} - 1) \left(\sum_{j \neq k} \check{\mathbf{h}}_k \mathbf{Q}_j \check{\mathbf{h}}_k^H + N_0 \right); \\
& \sum_{k=1}^{K} \text{tr}\{\mathbf{Q}_k \mathbf{A}_n\} \leq P_n. \quad (41)
\end{aligned}
$$

Problem (41) is convex and can be solved numerically [27]. Therefore, the seemingly non-convex feasibility problem (40) can be efficiently solved, so that the polyblock algorithm [21] can be applied to find the optimal rate-tuple. In more detail, for an upper-bound rate-tuple $\hat{\mathbf{r}}^{outer}$, we can always find a point on the boundary of the achievable rate region expressed as $t^{opt}\hat{\mathbf{r}}^{outer}$, where $t^{opt} \in [0, 1)$ is obtained by applying the bisection method on t to check whether problem (41) is feasible with $t\hat{\mathbf{r}}^{outer}$. In such way, each UE's upper-bound rate $\hat{r}_k^{outer}$ can be individually replaced by a feasible one $t\hat{r}_k^{outer}$, thus $\hat{\mathbf{r}}^{outer}$ can be gradually refined until the optimal rate-tuple is found, which is achievable with a gap of ε.

APPENDIX II
PROOF OF THEOREM 1

In order to generate the upper-bound rate for UE k, first, the BS needs to terminate the service with the other $K - 1$ UEs because any transmission to a UE other than UE k will in no way increase the signal power of UE k and will incur inter-UE interference to UE k, leading to a sub-optimal rate. Second, the BS should pour all its transmission power P onto UE k since saving power will just decrease the signal strength received at

UE k. Thus, we should concentrate on the signal part of UE k and write the beamforming vector for UE k in a general form with full BS power as

$$\mathbf{w}_k = \sqrt{P}\tilde{\mathbf{w}}_k = \sqrt{P}\left(\beta_k\hat{\mathbf{h}}_k^{\mathrm{H}} + \sqrt{1-|\beta_k|^2}\mathbf{v}_k\right), \quad (42)$$

where $\mathbf{v}_k$ is a unit-norm vector orthogonal to $\hat{\mathbf{h}}_k^{\mathrm{H}}$ and β_k is a complex value satisfying $|\beta_k| \in [0, 1]$ to make $\tilde{\mathbf{w}}_k$ a normalized vector. According to (8) and (42), the expected signal power of UE k can be derived as in (43), shown at the bottom of the page.

In (43), equation (a) holds because Z, $\mathbf{e}_k^\diamond$, and $\mathbf{v}_k$ are independently distributed. Equation (b) is obtained from the fact that $\mathbf{e}_k^\diamond$, and $\mathbf{v}_k^{\mathrm{H}}$ are i.i.d. isotropic vectors located in the $(N-1)$-dimensional nullspace of $\hat{\mathbf{h}}_k$, and hence $|\mathbf{e}_k^\diamond\mathbf{v}_k|^2$ follows a beta$(1, N-2)$ distribution and its mean value is $1/(N-1)$ [28]. According to [6], $\mathbb{E}\{Z\}$ can be computed as

$$\mathbb{E}\{Z\} = 2^B\beta\left(2^B, \frac{N}{N-1}\right). \quad (44)$$

In (44), $\beta(x, y)$ is the beta function defined as $\beta(x, y) = (\Gamma(x)\Gamma(y))/(\Gamma(x+y))$ [28], where $\Gamma(\cdot)$ denotes the gamma function [28]. Since it is easy to verify that

$$1 - \frac{N}{N-1}\mathbb{E}\{Z\} > 0, \quad \text{for } N > 1, B \geq 0, \quad (45)$$

we can conclude that $\mathbb{E}\{S_k^\diamond\}$ in (43) is a monotonically increasing affine function with respect to $|\beta_k|^2$. Thus, $\mathbb{E}\{S_k^\diamond\}$ achieves its maximum value when $|\beta_k|^2 = 1$, and hence we have

$$\mathbb{E}\{S_k^\diamond\} \leq A_k^{\mathrm{ave}}P(1 - \mathbb{E}\{Z\}). \quad (46)$$

Finally, from (12), we can upper bound the expected rate for UE k as

$$\begin{aligned}
&\mathbb{E}\{\log_2(1 + SINR_k^\diamond)\} \\
&\leq \log_2(1 + \mathbb{E}\{SINR_k^\diamond\}) \\
&\leq \log_2\left(1 + \frac{\mathbb{E}\{S_k^\diamond\}}{N_0}\right) \\
&\leq \log_2\left(1 + \frac{A_k^{\mathrm{ave}}P(1 - \mathbb{E}\{Z\})}{N_0}\right).
\end{aligned} \quad (47)$$

Our proof is completed by plugging (44) into (47).

<div align="center">APPENDIX III
PROOF OF LEMMA 2</div>

With some mathematical manipulation, $(a + bZ)/(c + dZ)$ can be rewritten as

$$\frac{a+bZ}{c+dZ} = \frac{b}{d} + \frac{\frac{a}{c} - \frac{b}{d}}{1 + \frac{d}{c}z}. \quad (48)$$

First, d can be derived as

$$d = A_k^{\mathrm{ave}}\sum_{j\neq k}\tilde{P}_j\left(\frac{1}{N-1} - \frac{N}{N-1}|\beta_j|^2\right)$$

$$= A_k^{\mathrm{ave}}\left(\frac{\sum_{j\neq k}\tilde{P}_j}{N-1} - \frac{N}{N-1}\sum_{j\neq k}\tilde{P}_j|\beta_j|^2\right)$$

$$\geq A_k^{\mathrm{ave}}\left(\frac{\sum_{j\neq k}\tilde{P}_j}{N-1} - \frac{N}{N-1}\sqrt{\sum_{j\neq k}\tilde{P}_j^2\sum_{j\neq k}|\beta_j|^4}\right) \quad (49)$$

$$\geq A_k^{\mathrm{ave}}\left(\frac{\sum_{j\neq k}\tilde{P}_j}{N-1} - \frac{N}{N-1}\sqrt{\left(\sum_{j\neq k}\tilde{P}_j\right)^2\sum_{j\neq k}|\beta_j|^4}\right) \quad (50)$$

$$= A_k^{\mathrm{ave}}\left(\frac{\sum_{j\neq k}\tilde{P}_j}{N-1} - \frac{\sum_{j\neq k}\tilde{P}_j}{N-1}N\sqrt{\sum_{j\neq k}|\beta_j|^4}\right), \quad (51)$$

where (49) is obtained from the Cauchy-Schwarz inequality and (50) is valid because $\sum_{j\neq k}\tilde{P}_j^2 \leq (\sum_{j\neq k}\tilde{P}_j)^2$. From (51), we can conclude that $d \geq 0$ if $\sum_{j\neq k}|\beta_j|^4 \leq (1/N^2)$. Therefore, in the following, we consider two cases, i.e., $d = 0$ and $d > 0$.

$$\begin{aligned}
\mathbb{E}\{S_k^\diamond\} &= \mathbb{E}\{|\mathbf{h}_k\mathbf{w}_k|^2\} \\
&= A_k^{\mathrm{ave}}P\mathbb{E}\left\{\left|\tilde{\mathbf{h}}_k^\diamond\tilde{\mathbf{w}}_k\right|^2\right\} \\
&= A_k^{\mathrm{ave}}P\mathbb{E}\left\{(1-Z)|\beta_k|^2 + Z(1-|\beta_k|^2)|\mathbf{e}_k^\diamond\mathbf{v}_k|^2\right\} \\
&\quad + 2A_k^{\mathrm{ave}}P\mathbb{E}\left\{\Re\left\{\sqrt{(1-Z)Z(1-|\beta_k|^2)}\beta_k\mathbf{e}_k^\diamond\mathbf{v}_k\right\}\right\} \\
&\overset{(a)}{=} A_k^{\mathrm{ave}}P\mathbb{E}\left\{(1-Z)|\beta_k|^2 + Z(1-|\beta_k|^2)|\mathbf{e}_k^\diamond\mathbf{v}_k|^2\right\} \\
&\overset{(b)}{=} A_k^{\mathrm{ave}}P\left[(1-\mathbb{E}\{Z\})|\beta_k|^2 + \mathbb{E}\{Z\}(1-|\beta_k|^2)\frac{1}{N-1}\right] \\
&= A_k^{\mathrm{ave}}P\left[\frac{\mathbb{E}\{Z\}}{N-1} + \left(1 - \frac{N}{N-1}\mathbb{E}\{Z\}\right)|\beta_k|^2\right] \quad (43)
\end{aligned}$$

Case 1: $d = 0$

It is straightforward to show that

$$\mathbb{E}_{[Z]}\left\{\frac{a + bZ}{c + dZ}\right\} = \mathbb{E}_{[Z]}\left\{\frac{a + bZ}{c}\right\}$$

$$= \frac{\mathbb{E}_{[Z]}\{a + bZ\}}{c}$$

$$= \frac{\mathbb{E}_{[Z]}\{a + bZ\}}{\mathbb{E}_{[Z]}\{c + dZ\}}. \tag{52}$$

Case 2: $d > 0$

If $|\beta_k|^4 \geq (1/N^2)$, it is apparent that $b \leq 0$ since $b = A_k^{\text{ave}}\bar{P}_k((1/(N-1)) - (N/(N-1))|\beta_k|^2)$ from (26). Besides, it is easy to show that $a, c > 0$ from the definition in (26). Hence, in (48), $(a/c) - (b/d) > 0$ since $a, c, d > 0$ and $b \leq 0$, which leads to the convexity of $((a/c) - (b/d))/(1 + (d/c)z)$ for $z > 0$. Hence, the following inequality holds,

$$\mathbb{E}_{[Z]}\left\{\frac{\frac{a}{c} - \frac{b}{d}}{1 + \frac{d}{c}z}\right\} \geq \frac{\frac{a}{c} - \frac{b}{d}}{\mathbb{E}_{[Z]}\left\{1 + \frac{d}{c}z\right\}}. \tag{53}$$

Plugging (53) into (48) yields

$$\mathbb{E}_{[Z]}\left\{\frac{a + bZ}{c + dZ}\right\} \geq \frac{b}{d} + \frac{\frac{a}{c} - \frac{b}{d}}{\mathbb{E}_{[Z]}\left\{1 + \frac{d}{c}z\right\}}$$

$$= \frac{b\mathbb{E}_{[Z]}\{Z\} + a}{\mathbb{E}_{[Z]}\{c + dZ\}}$$

$$= \frac{\mathbb{E}_{[Z]}\{a + bZ\}}{\mathbb{E}_{[Z]}\{c + dZ\}}. \tag{54}$$

Our proof is thus concluded from (52) and (54).

ACKNOWLEDGMENT

REFERENCES

[1] D. Gesbert, M. Kountouris, R. Heath, C. Chae, and T. Salzer, "From single-user to multiuser communications: Shifting the MIMO paradigm," *IEEE Signal Process. Mag.*, vol. 24, no. 5, pp. 36–46, Sep. 2007.

[2] G. Caire and S. Shamai, "On the achievable throughput of a multiantenna Gaussian broadcast channel," *IEEE Trans. Inf. Theory*, vol. 49, no. 7, pp. 1691–1706, Jul. 2003.

[3] T. Yoo and A. Goldsmith, "On the optimality of multianntenna broadcast scheduling using zero-forcing beamforming," *IEEE J. Sel. Areas Commun.*, vol. 24, no. 3, pp. 528–541, Mar. 2006.

[4] M. Sharif and B. Hassibi, "A comparison of time-sharing, DPC, beamforming for MIMO broadcast channels with many users," *IEEE Trans. Commun.*, vol. 55, no. 1, pp. 11–15, Jan. 2007.

[5] *Evolved Universal Terrestrial Radio Access (E-UTRA): Physical Layer Procedures*, 3GPP TS 36.213 V11.2.0, Feb. 2013.

[6] N. Jindal, "MIMO broadcast channels with finite-rate feedback," *IEEE Trans. Inf. Theory*, vol. 52, no. 11, pp. 5045–5060, Nov. 2006.

[7] M. Botros and T. Davidson, "Convex conic formulations of robust downlink precoder designs with quality of service constraints," *IEEE J. Sel. Topics Signal Process.*, vol. 1, no. 4, pp. 714–724, Dec. 2007.

[8] C. Zhang, W. Xu, and M. Chen, "Robust MMSE beamforming for multiuser MISO systems with limited feedback," *IEEE Signal Process. Lett.*, vol. 16, no. 7, pp. 588–591, Jul. 2009.

[9] M. Sadek, A. Tarighat, and A. Sayed, "A leakage-based precoding scheme for downlink multi-user MIMO channels," *IEEE Trans. Wireless Commun.*, vol. 6, no. 5, pp. 1711–1721, May 2007.

[10] B. Dai, W. Xu, and C. Zhao, "Multiuser beamforming optimization via maximizing modified SLNR with quantized CSI feedback," in *Proc. WiCOM, Netw. Mobile Comput.*, Sep. 2011, pp. 1–5.

[11] H. Du and P. Chung, "A probabilistic approach for robust leakage-based MU-MIMO downlink beamforming with imperfect channel state information," *IEEE Trans. Wireless Commun.*, vol. 11, no. 3, pp. 1239–1247, Mar. 2012.

[12] P. Chung and H. Du, "Robust SLNR downlink beamforming based on Markov's inequality," in *Proc. IEEE ICC*, Jun. 2012, pp. 3627–3631.

[13] J. Zou, W. Liu, M. Ding, H. Luo, and H. Yu, "Transceiver design for AF MIMO two-way relay systems with imperfect channel estimation," in *Proc. IEEE GLOBECOM*, Dec. 2012, pp. 1–5.

[14] Z. Wang, W. Chen, and J. Li, "Efficient beamforming for MIMO relaying broadcast channel with imperfect channel estimation," *IEEE Trans. Veh. Technol.*, vol. 61, no. 1, pp. 419–426, Jan. 2012.

[15] A. Tajer, N. Prasad, and X. Wang, "Robust linear precoder design for multi-cell downlink transmission," *IEEE Trans. Signal Process.*, vol. 59, no. 1, pp. 235–251, Jan. 2011.

[16] R. Bhagavatula and R. Heath, "Adaptive limited feedback for sum-rate maximizing beamforming in cooperative multicell systems," *IEEE Trans. Signal Process.*, vol. 59, no. 2, pp. 800–811, Feb. 2011.

[17] W. Yu and T. Lan, "Transmitter optimization for the multi-antenna downlink with per-antenna power constraints," *IEEE Trans. Signal Process.*, vol. 55, no. 6, pp. 2646–2660, Jun. 2007.

[18] "Smart and fast: Embracing the mobile broadband future," in *Proc. 3GPP TSG RAN Workshop REL Onwards*, Jun. 2012, pp. 1–16, RWS-120018.

[19] S. Sesia, I. Toufik, and M. Baker, *LTE: The UMTS Long Term Evolution*. Hoboken, NJ, USA: Wiley, 2009.

[20] J. Brehmer and W. Utschick, "Utility maximization in the multi-user MISO downlink with linear precoding," in *Proc. IEEE ICC*, Jun. 2009, pp. 1–5.

[21] A. Rubinova, H. Tuyb, and H. Maysa, "An algorithm for monotonic global optimization problems," *Optimization*, vol. 49, no. 3, pp. 205–221, 2001.

[22] L. Liu, R. Zhang, and K. Chua, "Achieving global optimality for weighted sum-rate maximization in the K-user Gaussian interference channel with multiple antennas," *IEEE Trans. Wireless Commun.*, vol. 11, no. 5, pp. 1933–1945, May 2012.

[23] Y. Taesang, N. Jindal, and A. Goldsmith, "Multi-antenna downlink channels with limited feedback and user selection," *IEEE J. Sel. Areas Commun.*, vol. 25, no. 7, pp. 1478–1491, Sep. 2007.

[24] W. Santipach and M. Honig, "Asymptotic capacity of beamforming with limited feedback," in *Proc. IEEE ISIT*, Jun. 2004, p. 289.

[25] A. Wiesel, Y. Eldar, and S. Shamai, "Zero-forcing precoding and generalized inverses," *IEEE Trans. Signal Process.*, vol. 56, no. 9, pp. 4409–4418, Sep. 2008.

[26] J. Brehmer and W. Utschick, "Optimal interference management in multi-antenna, multi-cell systems," in *Proc. IZS Commun.*, Mar. 2010, pp. 134–137.

[27] M. Grant, S. Boyd, and Y. Ye, CVX User's Guide for cvx Version 1.1 (Build 565), Nov. 2007.

[28] I. Gradshteyn and I. Ryzhik, *Table of Integrals, Series, Products*, 7th ed. Amsterdam, The Netherlands: Elsevier, 2007.

[29] M. Bengtsson and B. Ottersten, "Optimal downlink beamforming using semidefinite optimization," in *Proc. 37th Annu. Allerton Conf. Commun., Control, Comput.*, Sep. 1999, pp. 987–996.

[30] E. Bjornson, N. Jalden, M. Bengtsson, and B. Ottersten, "Optimality properties, distributed strategies, measurement-based evaluation of coordinated multicell OFDMA transmission," *IEEE Trans. Signal Process.*, vol. 59, no. 12, pp. 6086–6101, Dec. 2011.

[31] Z. Luo, W. Ma, A. So, Y. Ye, and S. Zhang, "Semidefinite relaxation of quadratic optimization problems," *IEEE Signal Process. Mag.*, vol. 27, no. 3, pp. 20–34, May 2010.

[32] Y. Huang and D. Palomar, "Rank-constrained separable semidefinite programming with applications to optimal beamforming," *IEEE Trans. Signal Process.*, vol. 58, no. 2, pp. 664–678, Feb. 2010.

[33] J. Proakis, *Digital Communications*, 3rd ed. New York, NY, USA: McGraw-Hill, 1995.

[34] H. Wan and W. Chen, "Joint source and relay design for multi-user MIMO non-regenerative relay networks with direct links," *IEEE Trans. Veh. Technol.*, vol. 61, no. 6, pp. 2871–2876, Jun. 2012.

[35] M. Ding, J. Zou, Z. Yang, H. Luo, and W. Chen, "Sequential and incremental precoder design for joint transmission network MIMO systems with imperfect backhaul," *IEEE Trans. Veh. Technol.*, vol. 61, no. 6, pp. 2490–2503, Jul. 2012.

[36] X. Wang, W. Huang, S. Wang, J. Zhang, and C. Hu, "Delay and capacity tradeoff analysis for motioncast," *IEEE/ACM Trans. Netw.*, vol. 19, no. 5, pp. 1354–1367, Oct. 2011.

[37] X. Wang, L. Fu, and C. Hu, "Multicast performance with hierarchical cooperation," *IEEE/ACM Trans. Netw.*, vol. 20, no. 3, pp. 917–930, Jun. 2012.
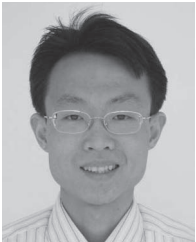
Ming Ding (M'12) received the B.S. and M.S. degrees (with first-class honors) in electronics engineering from Shanghai Jiao Tong University (SJTU), Shanghai, China, in 2004 and 2007, respectively. From September 2007 to September 2011, he pursued the Doctor in Philosophy (Ph.D.) with SJTU. In December 2011, he received the Ph.D. degree in signal and information processing from SJTU. In April 2007, he joined Sharp Electronics (Shanghai) Co., Ltd. Advance R&D Center [now Sharp Laboratories of China (SLC)] as a Researcher. From September 2007 to September 2011, he worked as a Researcher/Senior Researcher with SLC. He is currently a Principal Researcher with SLC. He has been working on B3G, 4G, and 5G wireless communication networks for more than 8 years and his research interests include OFDM synchronization, multiple-input multiple-output-OFDM technology, relay systems, interference management, cooperative communications, heterogeneous networks, device-to-device communications, and modeling of wireless communication systems. Up to now, he has published about 20 papers in IEEE journals and conferences, about 20 standardization contributions, as well as a Springer book on cooperative communications. In addition, as the first inventor, he holds 8 CN, 2 JP, and 2 KR patents and filed another 25+patent applications on 4G/5G technologies.

Hanwen Luo was born in 1950. Currently, he is a Professor in Shanghai Normal University, Shanghai, China and Shanghai Jiao Tong University, Shanghai. He is also the Vice-Director of the Shanghai Institute of Wireless Communications Technology with Shanghai Jiao Tong University. He used to be the leading Specialist of the China 863 high-tech program on Beyond 3G wireless communication systems and China 973 high-tech program on the researches of military equipment. His research interests include cooperative communications, multiple-input multiple-output-OFDM systems, etc.

Wen Chen (M'03–SM'11) received the B.S. and M.S. degrees from Wuhan University, Wuhan, China, in 1990 and 1993, respectively, and the Ph.D. degree from the University of Electro-Communications, Tokyo, Japan, in 1999. From 1999 to 2001, he was a Researcher of the Japan Society for the Promotion of Sciences (JSPS). In 2001, he joined the University of Alberta, Canada, starting as a Postdoctoral Fellow with the Information Research Laboratory and continuing as a Research Associate with the Department of Electrical and Computer Engineering. Since 2006, he has been a Full Professor with the Department of Electronic Engineering, Shanghai Jiao Tong University, China, where he is also the Director of the Institute for Signal Processing and Systems. Since 2014, he has served as the Dean of the School of Electronic Engineering and Automation, Guilin University of Electronic Technology. His interests cover network coding, cooperative communications, green communications, cognitive radio, and multiple-input single-output-OFDM systems. In this area, he has published 52 papers in IEEE Journals and more than 100 papers in IEEE conferences.